Chemical Geology 561 (2021) 120027

Contents lists available at ScienceDirect

Chemical Geology

journal homepage: www.elsevier.com/locate/chemgeo

# The role of low-temperature $^{18}O$ exchange in the isotopic evolution of deep subsurface fluids

Oliver Warr [a,*], Thomas Giunta [a], Tullis C. Onstott [b], Thomas L. Kieft [c], Rachel L. Harris [b,d], Devan M. Nisson [b], Barbara Sherwood Lollar [a]

[a] Department of Earth Sciences, University of Toronto, Toronto, ON, M5S 3B1, Canada
[b] Department of Geosciences, Princeton University, Princeton, NJ 08544, USA
[c] Biology Department, New Mexico Institute of Mining and Technology, Socorro, NM, USA
[d] Department of Organismic & Evolutionary Biology, Harvard University, Cambridge, MA 02138, USA

ARTICLE INFO

Editor: Michael E. Boettcher

ABSTRACT

Ca-Na-Cl fluids with high concentrations of dissolved reduced gases reside within fractures in crystalline Precambrian rocks around the world, and have been most intensively studied within South Africa, Fennoscandia and the Canadian Shield. In contrast to surface waters, shallow groundwaters, sedimentary basin brines and metamorphic fluids, the $\delta^{18}O$ and $\delta^{2}H$ values for these Ca-Na-Cl fluids typically plot to the left/above of the Global Meteoric Water Line (GMWL). To date, most interpretive frameworks for these fracture fluids have focused on their production via water-rock alteration reactions that affect both $\delta^{18}O$ and $\delta^{2}H$ values, resulting in co-variation of water isotope values above the GMWL. Such alteration processes include silicate hydration coupled with formation of secondary minerals, radiolytic $H_2$ formation, isotopic exchange with a $H_2$-rich gas, or isotope exchange with O and/or H-bearing minerals. This study presents the first compiled global isotopic dataset for these types of fluids, integrating a large amount of unpublished data with the previously published literature in order to investigate these fracture fluid systems on a global scale. Importantly this global perspective allows differentiation between fluids impacted by late-stage mixing with meteoric waters, from fluids that reflect the most saline end-members stored in the host rocks in hydrogeologic isolation from the surface hydrologic cycle. The most saline fluids are shown to occupy a more restricted range of $\delta^{18}O$-$\delta^{2}H$ space than previously recognised, with end-member fluids from all of the Precambrian rock settings investigated occupying a range of $\delta^{2}H$ $\delta^{18}O$ isotope space within which there is no co-variation in these values. These findings suggest a set of common processes may define the isotopic signatures of these most saline end-member fluids in Precambrian settings around the world – creating common signatures identifiable in these fluids, despite differences in geologic setting. This study identifies the important role of oxygen isotopic exchange between primary fluids (associated with hydrothermal/metamorphic activity) and the host rocks, taking place under low temperature, low-volume, water-rock ratios over long (Ma) geologic timescales. This process results in progressive $^{18}O$ depletion in the fluids over time, while $\delta^{2}H$ values remain less affected. For each site the specific isotopic signature of the fracture fluid end-member depends on initial hydrothermal/metamorphic fluid composition, rates of isotopic exchange, water-to-rock ratios, and in-situ residence times. We suggest the often-observed co-variation in both $\delta^{18}O$-$\delta^{2}H$ above the GMWL primarily results from late stage mixing of the fracture fluid end-members with (paleo)-meteoric water, resulting in isotopic regression back towards the GMWL, with end-points defined by the local meteoric-climatic conditions for each site.

## 1. Introduction

Within crystalline rocks of the Precambrian continental crust around the world, highly saline fracture waters have been identified, and most intensively studied to date within South Africa, Fennoscandia and the Canadian Shield (e.g. Frape and Fritz, 1982; Nurmi et al., 1988; Bottomley et al., 2003; Frape et al., 2003; Kieft et al., 2005; Lin et al., 2006; Onstott et al., 2006; Stotler et al., 2012; Kietäväinen et al., 2013; Telling

* Corresponding author.
*E-mail address:* oliver.warr@utoronto.ca (O. Warr).

https://doi.org/10.1016/j.chemgeo.2020.120027
Received 16 October 2020; Received in revised form 10 December 2020; Accepted 11 December 2020
Available online 14 December 2020

et al., 2018; Heard et al., 2018). Saline fluids in this geologic setting range from Na-Cl-type near the surface, to more Ca-Na-Cl dominated fluids at depth, with salinity ranging from 60 up to 325,000 mg/L (A1 of the accompanying S.I.). Salinity, or Total Dissolved Solids (TDS), gradients typically co-vary with isotopic gradients such that the most saline samples at each locality are depleted in $\delta^{18}O$ and/or enriched in $\delta^{2}H$ relative to the Global Meteoric Water Line (GMWL), resulting in them plotting to the left/above the GMWL (Frape and Fritz, 1982; Frape et al., 1984, 2003, Sherwood Lollar et al., 1993; Kloppmann et al., 2002; Ward et al., 2004; Onstott et al., 2006; Kietäväinen et al., 2013). This contrasts with other saline subsurface fluids such as those found in sedimentary basins, or those interpreted to be metamorphic, which typically lie to the right/below the GMWL (e.g. Sheppard, 1986; Kharaka and Hanor, 2003, and references therein). The processes resulting in the Precambrian hosted saline fluids plotting above the GMWL remain a subject of active debate. Typically, a variety of mechanisms are invoked to account for the isotopic composition of these fluids, including hydrogen isotopic exchange with a $H_2$-bearing gas phase out of equilibrium with the water (e.g. $H_2S$), formation of $H_2$ and/or $O_2$ gases from the water, hydration of primary silicates coupled with formation of secondary minerals (e.g. carbonates, clay minerals, iron hydroxides) producing co-variation in $\delta^{2}H$ and $\delta^{18}O$ (Kloppmann et al., 2002 and references therein), and lastly isotope exchange with oxygen- and/or hydrogen-bearing minerals (e.g. Blomqvist, 1990; Clark and Fritz, 1997; Frape et al., 2003, 2014; Kieft et al., 2005; Onstott et al., 2006; Clark, 2015). A general schematic for these proposed mechanisms is displayed in Fig. 1 (along with the typical processes such as evaporation and high temperature exchange that result in the isotopic composition of waters falling below the GMWL).

Despite the identification of relevant mechanisms (Fig. 1), at most localities, the relative importance of the proposed mechanisms and hence the quantitative controls on isotopic signatures that plot above and to the left of the GMWL remain unresolved. Based primarily on bromine and chlorine ratios, some authors had speculated that saline fluids in the Canadian Shield crystalline basement could be due to evaporation of surface water, and/or freezing of seawater, prior to infiltration (e.g. Frape and Fritz, 1982; Herut et al., 1990; Bottomley et al., 1994, 1999; Starinsky and Katz, 2003; Greene et al., 2008). But more recent studies such as Stotler et al. (2012) and Kietäväinen et al. (2013) both independently concluded that saline fluid formation at depth through freezing is inconsistent with the physical and geochemical data available for the Canadian and Fennoscandian Shields. For most localities, a variety of potential mechanisms remain plausible

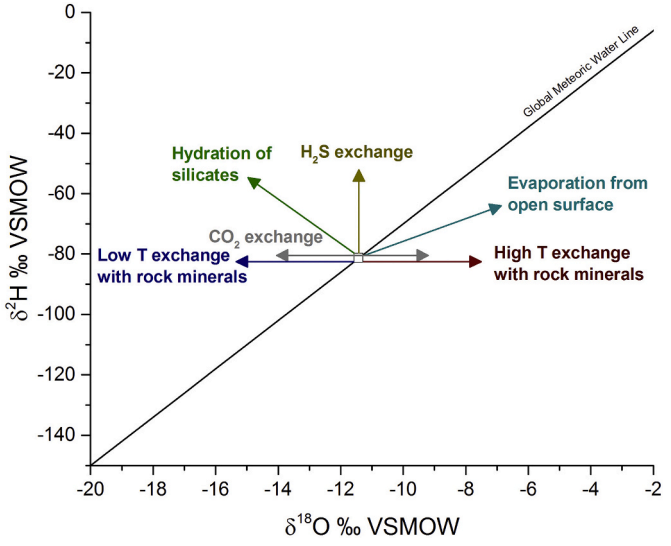


**Fig. 1.** Subsurface processes that can affect the $\delta^{2}H$ and $\delta^{18}O$ isotopic signature of groundwater. Figure modified from Clark and Fritz (1997).

(Fig. 1), but the relative importance of the proposed mechanisms and hence the quantitative controls on isotopic signatures that plot above and to the left of the GMWL remain a matter of debate.

In particular, the origin of primary fluid components prior to, and post, incorporation into the fracture networks remain uncertain in most cases, with no clear consensus reached on whether the primary source of the dissolved species (here termed salinity) is due to incursion of saline fluids from surface, or is primarily internally-generated in the host rocks (Nurmi et al., 1988; Frape et al., 2003, 2014; Onstott et al., 2006). External origins for the salinity include an incorporated seawater or terrestrial saline component (White, 1965; Bottomley et al., 1994; Frape et al., 2003; Greene et al., 2008; Landes et al., 2015) or dissolution of evaporite deposits (Fontes et al., 1989; Frape et al., 2003), depending on the location, depth and host rock. Proposed internal sources involve in situ water-rock interactions, typically either dissolution and alteration of host minerals (e.g. Fritz and Frape, 1982; Nurmi et al., 1988; Blomqvist, 1990; Kloppmann et al., 2002; Onstott et al., 2006; Kietäväinen et al., 2013), with potential influences from fluid inclusions contained within the host rock matrix (Garrels, 1984; Nordstrom et al., 1989; Lippmann-Pipke et al., 2011). Additionally, the existing salinity may be increased by water loss via reactions with host rock mineralogy or radiolysis (Vovk, 1987; Bucher and Stober, 2000; Kullerud, 2000; Kloppmann et al., 2002; Lin et al., 2005). A coherent theme in all the literature is that extensive water-rock reactions over geologically long timescales have obscured primary geochemical and isotopic features of the fluids, making identification of "source" fluids challenging.

This study integrates previously published data (376 points) with 216 new data points to establish a global dataset of $\delta^{18}O$ and $\delta^{2}H$ values for fracture fluids from the South African Kaapvaal craton, and the Fennoscandian and Canadian Shields – including novel data from some of the deepest and most ancient saline fluids identified to date – from 2.4 and 2.9 km below surface at the Kidd Creek Mine, Timmins, Ontario, Canada. The Kidd Creek brines in particular, shown to be hydrogeologically isolated in the deep subsurface on long geologic timescales with mean residence times of millions to more than a billion years based on noble gases (Holland et al., 2013; Warr et al., 2018), allow the most highly saline and deepest end-members from Precambrian shield settings to be more effectively constrained than in previous studies. As such, this study focuses in some detail on the fracture fluid samples collected from Kidd Creek, since the dedicated subsurface scientific observatory at Kidd Creek, in continuous operation since 2008, means it contains some of the most well characterized geochemical, isotopic and geological context for Precambrian Shield sites in this global dataset. Hosted in Kidd Creek Mine, the deepest base metal mine in North America, this Cu-Ag-Zn deposit is a stratiform Volcanogenic Massive Sulphide (VMS) deposit of 2.7 Ga age (Thurston et al., 2008) located 24 km north of the town of Timmins, Ontario Canada. Part of the Abitibi greenstone belt, the deposit is a massive hydrothermal system analogous to modern day black smoker vent systems on the ocean floor. Originally was laid down horizontally on the ocean floor where rising high temperature silica and metal-rich hydrothermal fluids mixed with infiltrating low temperature seawater, the Kidd-Munro assemblage consists of a series of now steeply dipping interlayered felsic, mafic, ultramafic and metasedimentary units (Bleeker and Parrish, 1996). During the last major regional metamorphic event at 2.67–2.69 Ga metamorphism reached a maximum of greenschist facies, followed by low-grade metamorphic hydrothermal events with peak temperatures of between 300 °C and ~ 220 °C at 2.64 Ga (Smith et al., 1993; Bleeker et al., 1999). The system has been continuously cooling since that time with estimated temperatures below 100 °C for the past two billion years (Li et al., 2016), making this one of the best-preserved sections of Precambrian hydrothermal deposition, with relict "pillow lava" structures still visible in the wall rock.

## 2. Sample collection and analysis

The $\delta^{18}O$ and $\delta^{2}H$ data for 592 fluid samples in this study from fracture networks in Precambrian crystalline rocks are compiled from studies from the South African Kaapvaal Craton and the Fennoscandian and Canadian Shields (Table A1 of the accompanying S.I.). All samples were collected from boreholes drilled into crystalline rock (which intersect with fluid-bearing fractures) using three techniques, depending on the locality: pumping from surface boreholes, collection from boreholes drilled from surface using samplers actuated at depth, and underground sampling mines from free-flowing and in some cases, valved boreholes. Sampling is described in detail in the respective studies (Frape and Fritz, 1982; Frape et al., 1984; Kelly et al., 1986; Nurmi et al., 1988; Bottomley et al., 1990; Bottomley et al., 1994; Lippmann et al., 2003; Frape et al., 2003; Onstott et al., 2006; Stotler et al., 2009; Stotler et al., 2011; Kietäväinen et al., 2013; Lau et al., 2014; Miettinen et al., 2015; Lau et al., 2016; Li et al., 2016; Simkus et al., 2016; Kietäväinen et al., 2017; Telling et al., 2018; Heard et al., 2018, Warr et al., 2018; Lollar et al., 2019) but described briefly as follows.

For the samples collected by pumping from the boreholes drilled from surface, the methodology is described by Kietäväinen et al. (2013), Purkamo et al. (2013), Bomberg et al. (2015), and others. Target sampling depths were isolated using a series of inflatable packers, and any standing water removed by slow pumping at a rate which matched the flow of water into the borehole from the surrounding fracture network. After a period of 9–63 days (depending on the flow rates), purging was stopped and fluids in the borehole were considered representative of the in situ fracture networks intersecting the boreholes. These fluids were pumped to surface and collected for isotopic and geochemical analyses.

For sampling from boreholes drilled from surface by collecting samples at depth (i.e. without pumping), the methods outlined by Nurmi and Kukkonen (1986) and Sherwood Lollar et al. (1994) were used. Both of these methods are able to collect representative fluid samples at specific depths of a borehole using either polyamide tubing (Nurmi and Kukkonen, 1986) or pressurized sampling vessels (Sherwood Lollar et al., 1994) with shut-off valves at each end. Sampling devices were lowered into the borehole from the surface to the specified sampling depth, either slowly with the valves open to match the filling rate of the tube (Nurmi and Kukkonen, 1986), or at a greater rate with the valves closed until the depth of interest is reached at which point the valves open, pumps circulate the fluids and water entered the sampling vessel (Sherwood Lollar et al., 1994). In both sampling approaches, valves were then closed and the sampled fluids maintained under pressure until extraction at surface.

Finally, samples collected from free-flowing and valved boreholes within mines were taken directly at the borehole collars after the methods described in Sherwood Lollar et al. (2002) and Ward et al. (2004) and Lin et al. (2006). Briefly, a packer was inserted into the borehole below the water level and inflated to isolate the sample. After a period of flushing, samples were collected in Nalgene bottles with no headspace for isotopic analysis of $\delta^{18}O$ and $\delta^{2}H$. Anion and cation samples were filtered using a 0.2 μm filter and collected in a 60 mL Nanopure water washed Nalgene following the methods outlined in Ward et al. (2004), and Lollar et al. (2019). The cation sample bottles contained trace metal grade $HNO_3$ in vial to prevent precipitation of mineral phases. The specific analytical methods for previously published data are outlined in their respective publications. Where available, water isotope data from service water (waters introduced into the mine for use in drilling and mine operations) is provided in Table A2 to constrain the isotopic composition of any external fluids the mines pump underground, and to identify any potential fluid contamination from ongoing mining activity. Sources of such service waters vary between mines but can range from modern, meteoric water pumped from the surface (Lollar et al., 2019), to groundwaters from shallow aquifers overlying the mining operation (e.g. Onstott et al., 2006). Service waters typically have $\delta^{18}O$ and $\delta^{2}H$ distinct from those of the fracture fluids and hence can serve as a measure of the degree of mixing and/or contamination, if such is present (Li et al., 2016; Lollar et al., 2019).

### 2.1. $\delta^{18}O$ and $\delta^{2}H$ sample analysis

For previously unpublished data, the $\delta^{18}O$ and $\delta^{2}H$ values of the fluids were determined at the University of Waterloo using the MP-GVI-IsoPrime and EA/HT-Micromass-IsoPrime systems, respectively. Prior to analysis, the conductivity of groundwater samples was determined, and where conductivity was high (> 0.1 S/m), samples were pre-treated by azeotropic distillation as per established methods (Fritz et al., 1986; Horita and Gat, 1988). The $\delta^{18}O$ was determined by $CO_2$ equilibration using standard procedures based on the principles of Epstein and Mayeda (1953). The $\delta^{2}H$ was performed on $H_2$ produced from water reduced on hot chromium as per Morrison et al. (2001). Accuracy of analysis for both techniques is confirmed by analysing duplicates and comparison to international reference standards sourced from the International Atomic Energy Agency (IAEA). The analytical methodologies are outlined as follows.

The $\delta^{18}O$ for each fluid sample was determined by the MP-GVI-IsoPrime instrument as previously described in detail Ward et al. (2004), Warr et al. (2018) and others. Initially, septum vials were filled with 200 μL aliquots of each sample and flushed with a 2% $CO_2$-helium mixture. All the samples were then heated to 40 °C for a minimum of 3.5 h to allow complete oxygen isotopic equilibration between the $CO_2$ and the sample $H_2O$. Following this, the $CO_2$ in the headspace was automatically extracted using a Gilson Autosampler and GVI Multiprep combined automated sample preparation system. This setup separated $CO_2$, $N_2$, $O_2$ and $H_2O$ using a 500 μL sample column. A helium carrier gas then transferred the purified $CO_2$ to the IsoPrime continuous flow isotope ratio mass spectrometer system (CF-IRMS) where the oxygen isotope ratios are measured to a precision of ±0.2‰. Calibrations were done using international reference materials V-SMOW (Vienna Standard Mean Ocean Water) and V-SLAP (Vienna Standard Light Antarctic Precipitation) from the IAEA. All values are expressed with respect to V-SMOW.

For $\delta^{2}H$ the EA/HT-Micromass-IsoPrime mass spectrometer was used. For the analytical procedure, 0.2 μL of each fluid sample was first pipetted into 2 mL septum vials which were then placed into a CTC AS200 Auto-sampler (LAS). From here, each sample was sequentially injected into a heated inlet system where a helium carrier gas transported it to a Eurovector Euro 3000 Elemental Analyzer with a 960 °C chromium furnace where the water was reduced to hydrogen gas. The $H_2$ was again transported via helium carrier gas to the EA/HT-Micromass IsoPrime mass spectrometer, which determined the $\delta^{2}H$ value for the sample. The precision for this technique is given as ±0.8‰. Calibrations were done using international reference materials V-SMOW (Vienna Standard Mean Ocean Water) and V-SLAP (Vienna Standard Light Antarctic Precipitation) from the IAEA. All values are expressed with respect to V-SMOW.

### 2.2. Aqueous geochemistry

For salinity data from published data sets, the specific analytical methods of the previously published data are outlined in their respective publications. Where concentrations of dissolved species are given, these were summed to determine total dissolved solids (TDS) in mg/L and are provided alongside the respective water isotope data in Table A1. For previously unpublished samples, the concentrations of dissolved species were analyzed by Activation Laboratories Ltd. (ISO/ IEC 17025 certified) as previously outlined in Lollar et al. (2019). The cation content of the samples was measured using Spectro Cirros (ICP-OES) and their counterpart anion samples were analyzed using a DIONEX DX-120 Ion Chromatography System (Ion Chromatography). Analytical accuracy of the measured ionic species was checked by confirming samples had a charge balance error of less than 5% following the approach outlined in

Lollar et al. (2019).

## 3. Results

The isotopic data from Table A1 is plotted in Fig. 2(A–C) with respect to the GMWL for each region. As mentioned above, these fracture fluids typically fall above the GMWL relative to local meteoric water samples, and compared to service waters derived from local meteoric waters. Data which plot in between the GMWL and the most $\delta^2$H-enriched, $\delta^{18}$O-depleted values reflect to some extent a greater or lesser degree of mixing with meteoric waters either due to groundwater recharge from surface, or due to anthropogenic activities such as the aforementioned circulation of mine service waters (e.g. Frape and Fritz, 1982; Fritz and Frape, 1982; Bottomley et al., 1994; Clark and Fritz, 1997; Bottomley et al., 1999; Kloppmann et al., 2002; Frape et al., 2003, 2014; Ward et al., 2004; Onstott et al., 2006; Greene et al., 2008; Kietäväinen et al., 2013; Li et al., 2016). The degree to which the observed $^{18}$O—$^{2}$H co-variation at many of these sites (Fig. 2(A–C)) is controlled by such mixing with meteoric waters, versus controlled by water-rock reactions (WRI) has been more difficult to deconvolve however. Kloppmann et al. (2002)'s study of fluids from the Vienne granitic basement complex in France remains one of the few studies to quantitatively resolve the relative contributions of WRI and mixing to the $^{18}$O—$^{2}$H correlation trends in their data.

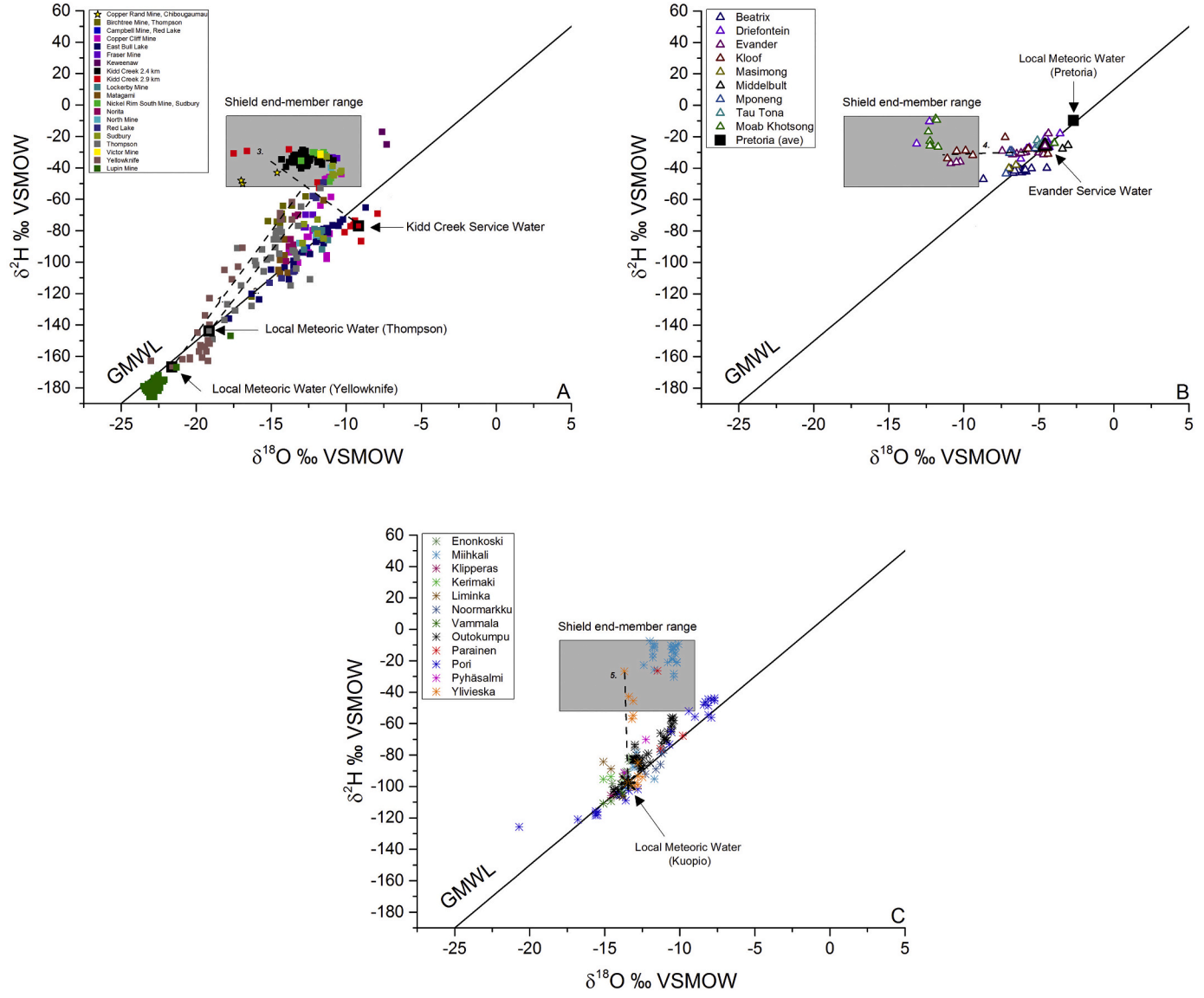


**Fig. 2.** Oxygen and hydrogen isotope data for fracture fluids from shield environments from Table A1 plotted relative to the Global Meteoric Water Line (GMWL). Data have been divided into the Canadian Shield (A, solid squares), South Africa (B, open triangles) and the Fennoscandian Shield (C, asterisks). Each site is colour-coded as per the key and is available in colour online. Errors for $\delta^2$H and $\delta^{18}$O are ±0.8 and ± 0.2‰ respectively and are smaller than the plotted symbols. The area shaded in grey is based on the range of $\delta^2$H and $\delta^{18}$O values for those fluids most elevated above the GMWL in Figures 2ABC, and encompasses end-members from all the shields (see text). For context, samples representative of local meteoric water (enlarged bold symbols) are plotted for two Canadian sites Yellowknife and Thompson, (A - Canada), for Pretoria (B - South Africa), and Kuopio (C - Finland), all from the IAEA WISER database (www.iaea.org). (Paleo)meteoric service water is also plotted from Evander Mine, South Africa (FB). Lastly, for Kidd Creek, a sample of mine service water (from a lake on the mine site) is also shown in (A). These examples of local meteoric water allow the figure to demonstrate in dashed lines 1–3 (Fig. 2A), and 4–5 (Fig. 2B and C respectively) how late-stage mixing between the elevated end-member crystalline shield saline fluids, and meteoric end-members recharged from surface can produce the observed spread of data. Line 1 (Yellowknife); Line 2 (Thompson), Line 3 (Kidd Creek); Line 4 (Evander and Kloof); Line 5 (Ylivieska). Also plotted in 2A are brine isotopic data from vugs measured by Guha and Kanwar (1987) from Copper Rand Mine, Canada (yellow stars) which are discussed in the main text. (For interpretation of the references to colour in this figure legend, the reader is referred to the web version of this article.)

In addition to the challenge of identifying the multiple mixing and WRI processes controlling isotopic distribution at the various sites, a major challenge has been identifying (to the degree possible in such highly altered systems), the fracture fluid end-members least affected by mixing with meteoric waters (most elevated over the GMWL). To date this has largely been done simply by extrapolating the linear $^{18}O$—$^{2}H$ correlation to a hypothetical end-member for a given locality (Frape et al., 1984; Kloppmann et al., 2002). In this study, by integrating the global data from three continents, it is possible to identify a common isotopic range of fracture fluids which lie most elevated above the GMWL and may for the first time provide empirical constraints for the previously hypothetical end-member. This range is highlighted by the shaded box in Fig. 2 which represents a $\delta^{2}H$-$\delta^{18}O$ range of −7 to −52‰ and − 18 to −9‰ respectively, and which includes fluids trapped in vugs formed from hydrothermal/metamorphic activity from Copper Rand Mine in the Canadian Shield (Guha and Kanwar, 1987). This range is comparable to hypothetical end-member ranges proposed by Frape and Fritz, (1982) and Bottomley et al. (1999).

Table 1 represents a global compilation of published noble gas-derived mean fluid residence times for fracture fluids in Precambrian crystalline rocks available to date for South Africa, Fennoscandia and the Canadian Shield for a subset of the samples in Table A1. Although variations exist in the approach and parameters used to calculate fluid residence times, from Table 1 it is clear that fracture fluids in Precambrian host rocks around the world have the documented potential to be geochemically isolated from modern surface hydrogeologic cycle on time scales ranging from hundreds of thousands, to millions and even in extreme cases, more than a billion years (see references in Table 1). In locations where fluids have the longest mean residence times (in the range of 100 Ma and above), such as Kidd Creek Mine, Fraser Mine, Nickel Rim, Yellowknife, Evander, and Kloof, the $\delta^{2}H$ and $\delta^{18}O$ values plot close to, or within the shaded empirical fracture fluid end-member range shown in Fig. 2. These end-member fluids, the oldest and most elevated above the GMWL for each site, also correspond to the most highly saline end-member fluids at each location (Table A1) demonstrating that high salinity and long residence times are associated with the most elevated $\delta^{2}H$ and $\delta^{18}O$ values for each locality.

Figs. 2–3 show that the co-variation in $\delta^{18}O$ and $\delta^{2}H$ values is consistent with mixing from these highly saline ancient fracture fluids, back towards less saline fluids located on the GWML (dashed lines). While the intersection with the GMWL differs for each site depending on the local meteoric water for each location, at the other end of the trends, the mixing lines from sites across the Canadian Shield as diverse as Yellowknife, Thompson, and Kidd Creek and even from the Fennoscandian sites and South Africa all converge towards the shaded range of $\delta^{18}O$ and $\delta^{2}H$ values in Fig. 2 (Frape et al., 1984; Bottomley et al., 1999; Onstott et al., 2006; Li et al., 2016; Telling et al., 2018; Warr et al., 2018). The identification of a globally similar $\delta^{18}O$-$\delta^{2}H$ range for these most saline fracture fluid end-members changes the focus for investigation of fractionation effects resulting from the water-rock reactions and provides an insight which we will demonstrate is helpful in deconvolving the effects of mixing versus WRI. While mixing trends show co-variation in $\delta^{18}O$-$\delta^{2}H$ over a wide range of values, variation within the highest salinity end-members are not characterized by $^{18}O$—$^{2}H$ correlation – but instead occupy a distribution that is more horizontal. Specifically, the shaded area shows a variation in $\delta^{18}O$ of ~10‰ (relative to total variation for meteoric waters observed globally on the order of ~30‰); versus a variation in only 45‰ in $\delta^{2}H$ for the shaded area (relative to total variation for meteoric waters globally on the order of ~400‰; Craig, 1961). Relative to typical ranges of $\delta^{18}O$-$\delta^{2}H$ for global waters (Craig, 1961), the highly saline, oldest fluids in the shaded region have a relatively smaller variation in $\delta^{2}H$ compared to $\delta^{18}O$. For the first time this dataset suggests that, once the effects of mixing are recognised based on the $^{18}O$—$^{2}H$ correlation back towards less saline end-members that intersect the GMWL, the variation within the highest salinity end-members is principally $\delta^{18}O$ variation. Hence consideration of the origin of these deep crustal fluids should focus on water-rock reactions that predominantly affect $\delta^{18}O$ values. This is a novel perspective compared to most previous literature which typically focused more heavily on water-rock reactions and processes that could produce a combined $^{18}O$—$^{2}H$ correlation in the resulting fluids.

## 4. Discussion

### 4.1. A process-based model for global variation in deep saline fracture fluids in Precambrian crust

The most well-known set of processes that strongly affect $\delta^{18}O$ values while having little or relatively little affect on $\delta^{2}H$ isotopic values involve low-temperature $^{18}O$ isotope exchange with host rocks. Such processes are known to overprint the original fluid isotopic signal and produce significant horizontal shifts (Fig. 1 – this work, Clark and Fritz, 1997; Clark, 2015). If the fluids' position above the GMWL is principally caused by a horizontal shift to the left, then the starting range for these fluids can be considered prior to any $^{18}O$ isotopic exchange. Given the wide range of values for $\delta^{2}H$ of (paleo-)meteoric waters documented on a global scale of more than 400‰ (Craig, 1961), and given the wide range of localities with different climatic and geologic histories sampled in this study, a "common" meteoric-like surface water range is unlikely as a "source" fluid and not further considered. What is common to all sites is they are located in crystalline basement rocks, which with different lithological and geologic histories nonetheless all formed originally from a combination of metamorphic and hydrothermal processes. In cases like Kidd Creek, which formed as a massive subseafloor hydrothermal deposit analogous to modern day "black smokers", "original" fluids were likely a mixture of hydrothermal/metamorphic fluids and infiltrating Archean seawater. On both the Canadian Shield and the Kaapval Craton, the deepest saline fluids with the longest residences time have in fact been shown to contain noble gases components that are isotopically similar to remnants of past regional metamorphic fluids (Lippmann-Pipke et al., 2011; Holland et al., 2013). While conservative elements like the noble gases may retain information on primary fluids, the multiple processes, extensive WRI and long timescales have, as mentioned previously, altered and over-written geochemical and isotopic information about what the "original or primary" fluid components were. Detailed studies of metabasalts and metasediments by Taylor (1974) and Sheppard (1977, 1986) published $\delta^{18}O$ and $\delta^{2}H$ ranges for metamorphic fluids globally (and magmatic, seawater and meteoric) and suggested, based on thermal history, mineralogy and defined fractionation curves, that a typical $\delta^{2}H$ range of ~ −20 to −65‰, and a $\delta^{18}O$ range of ~ + 5 to +25‰ could be estimated for metamorphic fluids since the late Precambrian at least, with few exceptions (e.g. a potential increase in $\delta^{2}H$ up to 0‰ if dehydration of oceanic crust is considered – Sheppard, 1986). This relative consistency in global estimates of $\delta^{2}H$ values for hydrothermal/metamorphic fluids in Precambrian settings likely reflects the relatively low isotopic variation of $\delta^{18}O$ and $\delta^{2}H$ in host lithologies on a global scale (Taylor, 1974; Taylor, 1978; Longstaffe and Gower, 1983; Clark and Fritz, 1997; Eiler, 2001).

For the Superior Province of the Canadian Shield in particular, from which 226 of the samples in this study were collected, Kerrich and Ludden (2000) estimated the range of $\delta^{18}O$ and $\delta^{2}H$ values for metamorphic fluids (based on bulk rock analyses) of between +4 to +25‰ and − 20‰ to −65‰ respectively from the Archean to the present day, consistent with the range suggested above by Taylor (1974). Very similar ranges have been estimated for metamorphic fluids for the Fennoscandian Shield (Piribauer et al., 2011; Kietäväinen et al., 2013) and the South African Kaapvaal craton (e.g. Kieft et al., 2005; Lin et al., 2006; Onstott et al., 2006; Zhao et al., 2006; Grové and Harris, 2010), and more generally (e.g. Clark and Fritz, 1997). While $\delta^{2}H$ values cannot be considered conservative, it is nonetheless notable that this estimated isotopic range for metamorphic fluids from the literature reviewed

**Table 1**
Mean fluid residence times in crystalline basement fluids from South Africa, Fennoscandia and the Canadian Shield. Residence times presented here were determined through noble gas analysis of the fluids and are a function of in situ production of radiogenic noble gases over time through radioactive decay of naturally occurring U, Th, and K in the host rock. Residence times represent the estimated time required to accumulate the measured radiogenic noble gas content of the fracture fluids based on the noble gas production parameters (see Ballentine and Burnard, 2002 and references therein). Calculated mean residence times are based on models that integrate porosity estimates, the efficiency of release of noble gases from the rock matrix, and, where highlighted, external fluxes of noble gases into the system. Overall model parameters are briefly described here and the original literature citations are provided for further information regarding site-specific geochemistry, external fluxes, and residence time calculations.

| Country | Location | Mean Fluid Residence time (Ma) | Model Parameters | Source |
|---|---|---|---|---|
| Finland | Outukumpu Deep Drill Hole | 17–58 | Closed system<br>100% release from rock matrix (He—Ar)<br>0.5% porosity | Kietäväinen et al. (2014) |
| Canada | Con Mine (Yellowknife) | 340 | Closed system<br>100% release from rock matrix (He)<br>1.0% porosity | Bottomley et al. (2005) |
| | | 54–425 | Closed system<br>100% release from rock matrix (He, Ar)<br>1.0% porosity | Greene et al. (2008) |
| Canada | Kidd Creek Mine 2.4 km | 1142–1655 | Closed system<br>100% release from rock matrix (He—Xe)<br>1.0% porosity | Holland et al. (2013) |
| | | 359–414 | Closed system<br>100% release from rock matrix (He—Xe)<br>1.0% porosity | Warr et al. (2018) |
| Canada | Kidd Creek Mine 2.9 km | 1622–1890 | Closed system<br>100% release from rock matrix (He—Xe)<br>0.88% porosity | Warr et al. (2018) |
| Canada | Nickel Rim Mine | 250–357 | Closed system<br>100% release from rock matrix (He—Xe)<br>1.1% porosity | Warr et al. (2018) |
| Canada | Fraser Mine | 544 | Closed system<br>100% release from rock matrix (He—Xe)<br>1.2% porosity | Warr et al. (2018) |
| Canada | Whiteshell Nuclear Research Establishment | 0.09–20 | Closed system<br>100% release from rock matrix (He)<br>1.0% porosity | Bottomley et al. (1984) |
| S. Africa | Mponeng Mine | 15.8–25 | External flux<br>100% release from rock matrix (He, Ar)<br>20–80% release (Xe)<br>1.0% porosity | Lin et al. (2006) |
| S. Africa | Beatrix Mine | 16–92 | Closed system<br>100% release from rock matrix (He, Ar)<br>20–42% release (Xe)<br>1.0% porosity | Lippmann et al. (2003) |
| | | 0.6–5.1 | External flux<br>100% release from rock matrix (He, Ar)<br>20–44% release (Xe)<br>1.0% porosity | Lippmann et al. (2003) |
| | | 3–14 | External flux<br>100% release from rock matrix (He, Ar)<br>20–44% release (Xe)<br>1.0% porosity | Lau et al. (2016) |
| | | 13–136 | Closed system<br>100% release from rock matrix (He—Xe)<br>0.7% porosity | Heard et al. (2018) |
| S. Africa | Evander Mine | 13–364 | Closed system<br>100% release from rock matrix (He, Ar)<br>40–100% release (Xe)<br>1.0% porosity | Lippmann et al. (2003) |
| | | 1.0–9.6 | External flux<br>100% release from rock matrix (He, Ar)<br>43–80% release (Xe)<br>1.0% porosity | Lippmann et al. (2003) |
| S. Africa | Kloof Mine | 21–170 | Closed system<br>100% release from rock matrix (He, Ar)<br>22–52% release (Xe)<br>1.0% porosity | Lippmann et al. (2003) |
| | | 2.7–21.1 | External flux<br>100% release from rock matrix (He, Ar)<br>23–55% release (Xe)<br>1.0% porosity | Lippmann et al. (2003) |
| S. Africa | Witwatersrand Basin | 40- $\geq$ 2000 (He—Ar) | 40 Ma from closed system<br>100% release from rock matrix (He—Ar)<br>0.1–0.8% porosity<br>2000 Ma from fluid inclusion Ne component | Lippmann-Pipke et al. (2011)<br>Lippmann-Pipke et al. (2011) |
| S. Africa | Masimong Mine | 39–97 | Closed system<br>100% release from rock matrix (He—Ar) | Heard et al. (2018) |

(*continued on next page*)

**Table 1** (*continued*)

| Country | Location | Mean Fluid Residence time (Ma) | Model Parameters | Source |
|---|---|---|---|---|
| | | | 47–100% release (Xe)<br>0.7% porosity | |
| | | 3.4–10.8 | External flux<br>100% release from rock matrix (He—Ar)<br>47–100% release (Xe)<br>0.7% porosity | Heard et al. (2018) |
| S. Africa | Driefontein Mine | 1.1–12 | Closed system<br>100% release from rock matrix (He—Xe)<br>2% porosity | Heard et al. (2018) |
| | | 0.2–0.69 | External flux<br>100% release from rock matrix (He—Xe)<br>2% porosity | Heard et al. (2018) |
| S. Africa | Tau Tona Mine | 0.77 | Closed system<br>100% release from rock matrix (He—Ar),<br>13–100% release (Xe),<br>0.7% porosity | Heard et al. (2018) |
| | | 0.1–1.2 | External flux<br>100% release from rock matrix (He—Ar),<br>13–100% release (Xe)<br>0.7% porosity | Heard et al. (2018) |
| S. Africa | Zondereinde Mine | 2.7–12 | Closed system<br>100% release from rock matrix (He—Xe)<br>0.05% porosity | Heard et al. (2018) |
| | | 0.006–0.047 | External flux<br>100% release from rock matrix (He—Xe)<br>0.05% porosity | Heard et al. (2018) |

above is very similar to the range of $\delta^2H$ values shown in the most saline end-members at the sites in this study (shaded area in Fig. 1). It is well known that $\delta^2H$ values are less likely to be affected than $\delta^{18}O$ values, due to the relatively small mineral bound-H reservoir in rocks (Kelly et al., 1986; Guha and Kanwar, 1987; Clark and Fritz, 1997; Onstott et al., 2006). Some small degrees of $^2H$-enrichment have been shown. For example, Kloppmann et al. (2002) calculated that 40% loss of water due to hydration of feldspars could feasibly account for a modest (~15‰) $^2H$ enrichment. Alternatively, where hydrous minerals already exist, hydrogen isotopic exchange may result in a small extent of $^2H$ enrichment (~20‰) (e.g. Kieft et al., 2005; Onstott et al., 2006). Concomitant with this isotopic evolution, increasing ionic content can also occur due to water-rock reactions including enrichments in $Cl^-$, trace metals and cations such as $Ca^{2+}$ through in situ radiolysis of water (e.g. Vovk, 1987; Lin et al., 2005) or through a series of high-low temperature reactions, mineral hydration, gradual contributions from fluid inclusions, and ion exchange with minerals of the host rocks (e.g. Frape and Fritz, 1982; Nordstrom et al., 1989; Clark and Fritz, 1997; Bucher and Stober, 2000; Kullerud, 2000), Frape et al., 2003, 2014; Bottomley et al., 2005; Clark, 2015). Presently, the details of the origin and evolution of the salinity component in these fracture fluids remains an active area of research. This study focuses for now solely on the $\delta^{18}O$ and $\delta^2H$ isotopic composition.

In contrast to the range of $\delta^2H$ values, the shaded area (Fig. 2) is significantly more depleted in $^{18}O$ than the literature estimates for metamorphic/hydrothermal fluids and rocks/metasediments for the Precambrian crust reviewed above. During cooling, mineral growth/precipitation and low temperature equilibration under low water-rock ratios are well known processes that can result in more depleted $\delta^{18}O$ values in the remaining fluid phase (Fig. 1) due to preferential incorporation of the lighter $^{16}O$ isotope into the water phase (e.g. Clark and Fritz, 1997). Where water to rock ratios are sufficiently low, the $\delta^{18}O$ of the fluids at equilibrium with the host rock will depend only on the $\delta^{18}O$ of the host rock (and the temperature), independent of the initial fluid $\delta^{18}O$ (Clark and Fritz, 1997; Clark, 2015). Low temperature water-rock reaction rates are sluggish (Clark and Fritz, 1997), hence such processes would require long timescales of water-rock interaction to facilitate sufficient low-temperature isotopic exchange. The long residence times of the fluids (Table 1) associated with the most elevated and highly saline fluids (Figs. 2 and 3) are consistent with the extended residence times required to drive isotopic exchange between the fluids and host rocks towards equilibrium, even under present-day temperatures. For example, Kieft et al. (2005) and Onstott et al. (2006) applied low temperature equilibration models to fracture fluids from the Kaapval craton to suggest that ~70–80% isotopic equilibration could account for the $\delta^{18}O$ (and $\delta^2H$) values observed in the most saline end-members there (assuming very low water-to-rock ratios). Progressive low temperature equilibrium was proposed by Guha and Kanwar (1987) to explain the $\delta^{18}O$ and $\delta^2H$ values of Ca-Na-Cl-rich brines (326–407 g/L TDS) in vugs from Copper Rand Mine on the Canadian Shield (Table A1; Fig. 2A). Given their location in cross fractures within the vein system, the vugs have a clear association with hydrothermal/metamorphic activity, and the vug fluids were considered to be related to the mineralisation of the ore body. From this, Guha and Kanwar (1987) proposed that after fluid emplacement at elevated temperatures (~250 °C), mineralisation and cooling resulted in a reduction in the water-rock ratios and progressive depletion in the $\delta^{18}O$ of the residual saline fluids, resulting in the vug fluids plotting to the left of the GMWL, though no quantification of the extent of equilibration was provided. This study, by integrating a 592-sample dataset from a broad spectrum of Precambrian shield sites around the world, demonstrates that low temperature isotopic equilibration between the host rocks and the fracture fluids is likely the dominant process controlling the isotopic composition of deep cratonic fluids on a global scale. The well-known trends of $\delta^{18}O$ and $\delta^2H$ covariation tend to reflect the effects of later stage mixing with meteoric and paleo-meteoric fluids.

### 4.2. Quantitative application of the conceptual model to Kidd Creek

By far the greatest density of the new data in Fig. 2 is derived from what are, to date, the oldest fluids discovered in the Precambrian crust – the fracture fluids from 2.4 to 2.9 km depth at Kidd Creek Mine in Timmins, Ontario with mean residence times of more than a billion years (Holland et al., 2013; Warr et al., 2018). This density of samples is due to the Kidd Creek Observatory, which has over the course of 13 years provided the infrastructure and opportunity to monitor a suite of discharging saline fluids, making this the world's most longstanding and deepest location for investigation of subsurface fluids and deep life in the crystalline basement (Lollar et al., 2019). Data from two levels of the observatory can be used to investigate the mechanisms controlling the

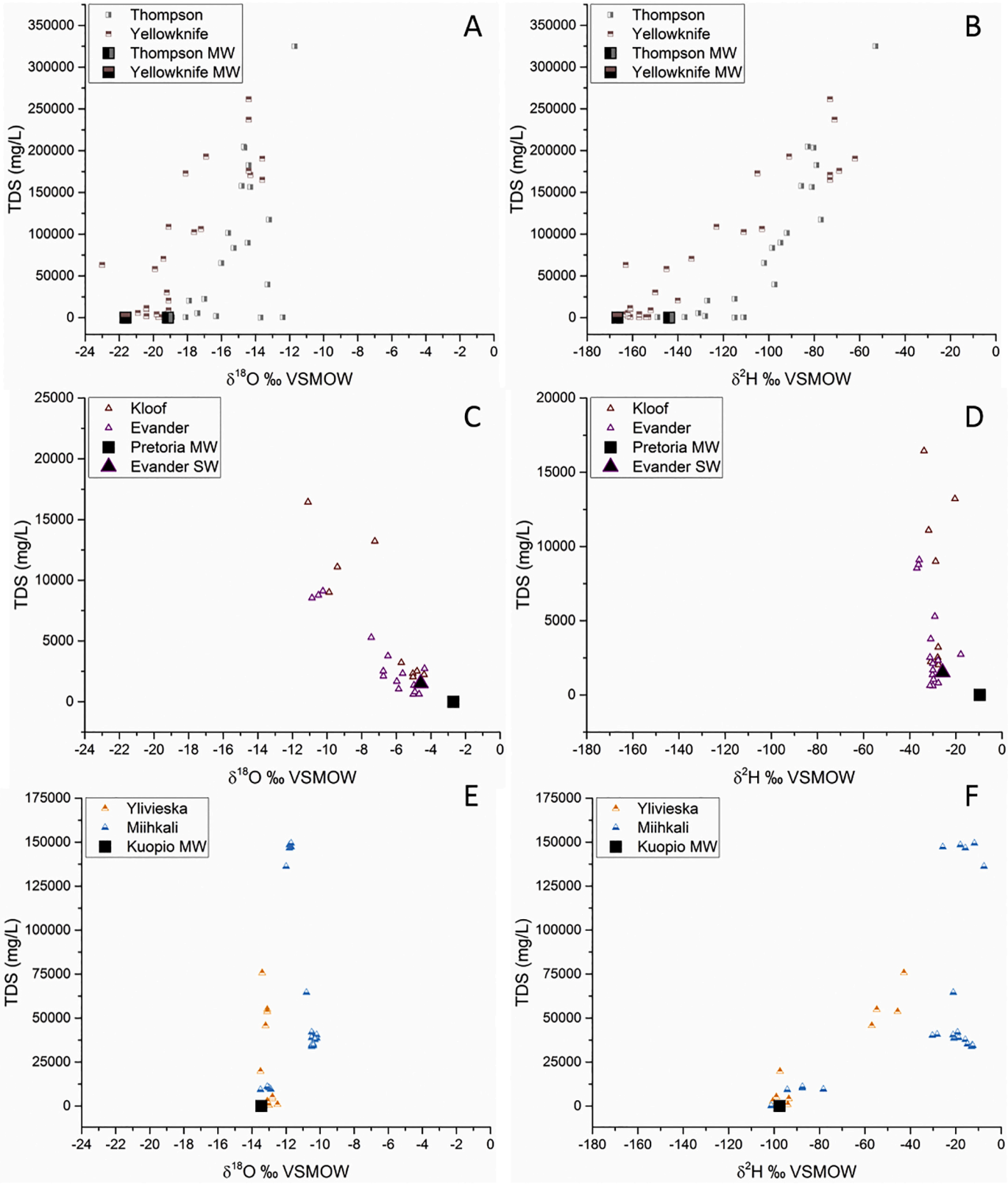


**Fig. 3.** Variation in total dissolved solid content (TDS) in the fluids with oxygen and hydrogen isotopic data for shield samples environments from Table A1. Data have been divided into the Canadian Shield (A-B), South Africa (C-D), and the Fennoscandian Shield (*E*-F). Each site is colour-coded as per the key and Fig. 2 and is available in colour online. Errors for $\delta^2H$ and $\delta^{18}O$ are ±0.8‰ and ± 0.2‰ respectively and are smaller than the symbols. For context, representative samples of local meteoric water (MW - enlarged bold symbols) are plotted for Yellowknife and Thompson, (Canada) for Pretoria (South Africa), and for Kuopio (Finland), from the IAEA WISER database (www.iaea.org). (Palaeo)meteoric Service water (SW) from Evander Mine, South Africa, is also plotted in C and D for context.

isotopic composition of the fracture waters in further detail. In Fig. 4, the data for Kidd Creek fracture fluids sampled at 2.4 km depth and 2.9 km depth (Table A1) are plotted alongside the service water that represents meteoric water used by the mining company for operations and drilling. This service water is sourced from a local lake, and as such has a slightly shallower gradient than typical GMWL slope, and plots along a line which intersects the GMWL with a classic 'lake water' slope (Lollar et al., 2019). As sampling at the 2.9 km level took place during a major drilling campaign, a significant proportion of the samples initially collected from 2.9 km are dominantly or significantly affected by recent addition of meteoric water during drilling, consistent with the lower salinities observed for these samples (Table A1). For example, the effect of meteoric water addition during mining at this level can be clearly observed in BH13762. The initial sample from this borehole plotted above the GMWL ($\delta^2$H of −29.3‰, $\delta^{18}$O of −16.6‰) with a TDS of 215,000 mg/L. However, the two successive samples showed that the TDS decreased by up to 99% and the isotopic composition plot along local meteoric line or else fall in a position intermediate between the GMWL and the average value for 2.9 km (shown by star in Fig. 4). This is consistent with the fact that these 2 samples were collected while the drill rigs were still in place in the holes (Table A1 of the accompanying S. I.). Three other samples from 2.9 km (shown in solid red circles) do not show this dilution with service waters and so have likely flushed out remnants of the drilling water fluid post-drilling completion.

Applying the conceptual model of low-temperature exchange to the specific example of the Kidd Creek data benefits from the very well characterized information available from the literature on the oxygen isotopic composition of the host rock and in particular, fracture minerals. In this locality, as typically observed elsewhere, calcite and quartz are the two most common and frequently observed fracture minerals and have been in prolonged contact with the water phase for extended time periods. Studies of quartz and calcite fracture minerals show the measured $\delta^{18}$O of both primary quartz and calcite fracture minerals associated with metamorphic fluids at Kidd Creek have an average $\delta^{18}$O value of ~12.0‰ (Kerrich et al., 1987; Huston and Taylor, 1999). Meanwhile, Kerrich and Ludden (2000) used bulk rock analyses to estimate a metamorphic fluid $\delta^{18}$O range of +6 to +9‰ at Kidd Creek. This range was independently supported by Huston and Taylor (1999) who inferred a similar $\delta^{18}$O range for metamorphic fluids of +6.7 to +7.0‰ from mineralogic studies. The same samples were also used to propose a tentative metamorphic fluid $\delta^2$H range of −9 to −26‰, which overlaps with the range of −20‰ to −65‰ considered for metamorphic fluids by Kerrich and Ludden (2000). These $\delta^{18}$O ranges were also consistent with estimated fluid $\delta^{18}$O values calculated from temperatures recorded from fluid inclusions and the $\delta^{18}$O of quartz and calcite from metamorphic veins elsewhere in the area (Beaty et al., 1988; Schandl and Wicks, 1991; Barrett et al., 2013) and are used as the basis for the shaded range (metamorphic fluid range) shown in Fig. 5.

Where a fluid-rock system reaches complete isotopic equilibrium under extremely low water-to-rock ratios, the relationship between equilibration temperature, the oxygen isotope fractionation (α) between the $\delta^{18}$O of each fracture mineral, and the fluid values ($^{18}O_{min}$and $\delta^{18}O_{H2O}$respectively) can be defined by the following equation:

$$\delta^{18}O_{H_2O} = \left(\frac{(1000 + \delta^{18}O_{min})}{\alpha_{min-water}(T)} - 1000\right) \quad (1)$$

Where the water-to-rock ratio is larger, and/or where isotopic exchange is incomplete, the relationship defined by Eq. 1 will not be valid. Instead,

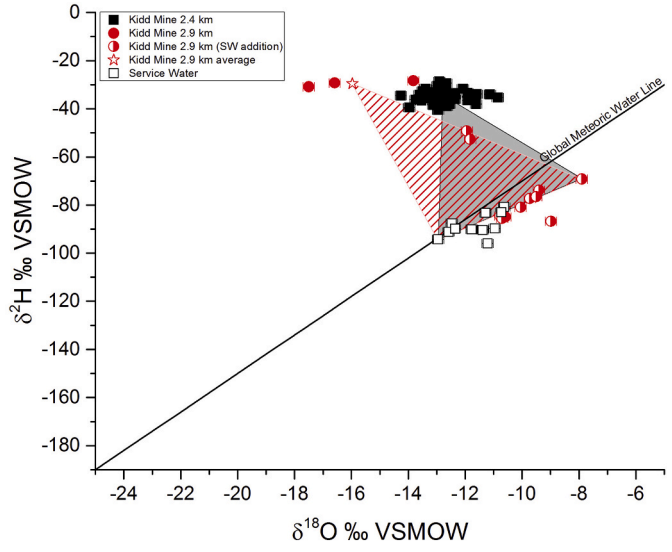


**Fig. 4.** Kidd Creek water isotope data for 2.9 km (red circles) compared with data from 2.4 km (black squares). While the $\delta^2$H is comparable between the two levels, there is a potential minor isotopic depletion in the $\delta^{18}$O of the water samples at the deeper level of the mine. This could simply be empirical as there are significantly more samples from the 2.4 km level versus the 2.9 km level to date. For both levels, a shaded region is shown that indicates where samples would fall if mixing were occurring between mine level average (star) and service water used within the mine. The lower slope line on which service waters fall was defined by Lollar et al. (2019). Only some samples from 2.9 km show a mixing effect, consistent with sample collection taking place while active drilling was still underway at this level. All but 5 of the samples from 2.9 km fall along the GMWL with 3 of these having comparable salinities to their 2.4 km counterparts (solid red circles) while 2 plotted within the shaded region. The majority of samples collected from 2.9 km are isotopically closer to the meteoric/service water line and reveal significantly lower salinities, consistent with the dilution effects of service water addition (symbols shown in half-white and half-red circles). The samples from 2.4 km are entirely isotopically distinct from the service waters. (For interpretation of the references to colour in this figure legend, the reader is referred to the web version of this article.)

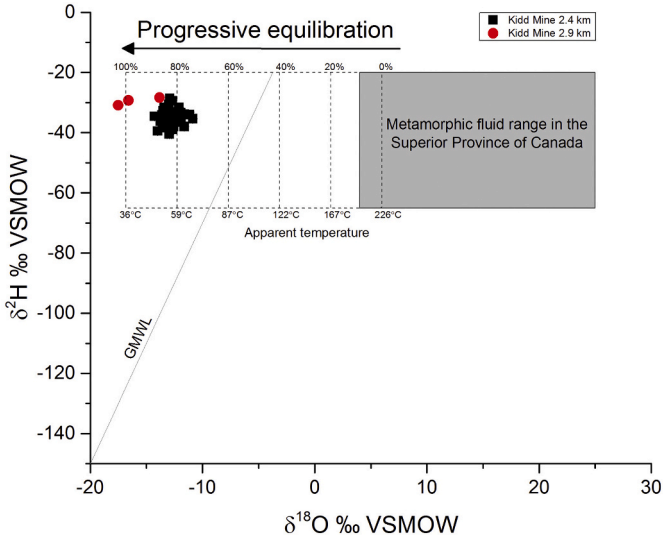


**Fig. 5.** Modelling isotopic evolution towards low-temperature equilibration between fracture water and quartz at 36 °C for Kidd Creek using isotope data for 2.9 km (red circles) compared with data from 2.4 km (black squares). Estimated metamorphic fluid values for the Canadian Shield are shown in the shaded region based on a $\delta^{18}$O value of 6‰ proposed for Kidd Creek by Kerrich and Ludden (2000) and the range estimated for $\delta^{18}$O and $\delta^2$H in the Superior Province of Canada (+4 to +25‰ and − 20‰ to −65‰ respectively) from Kerrich and Ludden (2000). This range is consistent with the typical metamorphic range for these types of fluid defined by Taylor (1974) based on metabasalts and metasediment data. The degree of isotopic fractionation between 0 and 1 is given as a percent along the top axis along with the apparent temperature the progressive fractionation corresponds provided for reference along the bottom. (For interpretation of the references to colour in this figure legend, the reader is referred to the web version of this article.)

Eq. 1 can be modified to evaluate the effect of progressive equilibration with the host mineralogy under low water-to-rock ratios after the approach outlined by Karolytė et al. (2017):

$$\delta^{18}O_{H_2O} = \left(\frac{(1000 + \delta^{18}O_{min})}{\alpha_{min-water}(T)} - 1000\right) \times f + \delta^{18}O_{H_2O(INIT)} \times (1 - f) \quad (2)$$

where $\delta^{18}O_{H2O}$ and $\delta^{18}O_{min}$ and represent the $\delta^{18}O$ of the fracture fluid and fracture mineral respectively, $\alpha_{min-water}(T)$ is the isotopic fractionation between the fracture mineral and fracture fluid at temperature T, $f$ is the fluid fraction that has equilibrated and $\delta^{18}O_{H2O(INIT)}$ is the initial metamorphic fluid value. In this model $\delta^{18}O_{min}$ is considered constant given the low water to rock ratios (following the method of Clark and Fritz (1997) and Clark (2015)).

Using the above equations, it is possible to evaluate the degree of equilibrium reached between the fracture fluids and the fracture minerals. Taking quartz as an example, at Kidd Creek, this fracture mineral has an average $\delta^{18}O$ value of 12.0‰ which has been estimated based on 10 analyses (Huston and Taylor, 1999), and the corresponding $\alpha_{(qz\text{-}water)}$ value can be determined using the temperature-dependent fractionation factors of Knauth and Epstein (1976) and Kawabe (1978). Here, a temperature of 36 °C is used based on a depth of 3 km and a geothermal gradient of 12 °C/km for this region of the Canadian Shield (Artemieva and Mooney, 2001; Warr et al., 2019).The initial metamorphic fluid $\delta^{18}O$ value of 6‰ for Kidd Creek is taken from the literature along with the proposed metamorphic fluid $\delta^{2}H$ range of −20‰ to −65‰ used by Kerrich and Ludden (2000) for the Superior Province. By increasing $f$ from 0 to 1 the progressive isotopic evolution towards equilibrium between the fracture fluids and the associated quartz under extremely low water-to-rock-ratios can be modelled. This is shown in Fig. 5.

Fig. 5 suggests fracture fluids collected from Kidd Creek for this study approach complete low-temperature equilibrium with the surrounding quartz fracture minerals. Though it is possible that the deeper level of the mine (2.9 km) may be slightly closer to complete equilibrium for infinitely low water-rock ratios, this cannot be conclusively confirmed based on the available data since as noted above, there are substantially more samples from 2.4 km than from 2.9 km.

Using the same approach, the relationship between calcite fracture mineralogy and the fracture fluids at Kidd Creek can also be evaluated using the temperature-dependent fractionation factor of O'Neil et al. (1969) and an estimated average fracture calcite $\delta^{18}O$ value of 12‰ ($n$ = 16, Kerrich et al., 1987). Incorporating this into Eq. 2, it can be seen that all Kidd Creek fluid samples indicate upwards of 80% equilibrium has also been reached between the fluids and the corresponding calcite fracture minerals. This again, suggests that the system is approaching low temperature equilibrium under low water to rock conditions. For the deeper 2.9 km samples though, equilibrium with calcite alone cannot produce the two most isotopically depleted fluid $\delta^{18}O$ values; this therefore may suggest $^{18}O$ exchange with quartz is the more dominant exchange mechanism affecting these fluid samples, (as highlighted by Fig. 5) with additional variation potentially due to variability in the local water/rock ratio.

Overall, four lines of evidence support an approach to complete oxygen isotopic equilibration between the fluids and the surrounding host rocks. The first is the good agreement for both carbonate-fluid; and quartz-fluid isotopic systems. It would be rather serendipitous for them to both have comparable isotopic fractionations which both reflect a system approaching isotopic equilibrium. Secondly, literature estimate of the water-to-rock ratio for these crystalline basement settings were summarized by Holland et al. (2013) and further, calculated by Sherwood Lollar et al. (2014), using an adapted model of Bethke (1985), yields ratios of approximately 0.01, which are consistent with the low water to rock ratios required for equilibration between the water phase and the host rock to be approached. Such low water-to-rock ratios are common for these environments as highlighted in Table 1. Third, the thermal history of the Kidd Creek system indicates temperatures have been below 100 °C for ~2 Ga (Li et al., 2016). Fourth, coupled with the previous point, noble gas dating of these fluids highlights that they have been isolated in situ over Ma to Ga timescales (Holland et al., 2013; Warr et al., 2018). Accordingly, there has likely been sufficient time for the mineral-fluid system to have equilibrated at ≤60 °C and resulted in progressive $^{18}O$ depletion in the fluids.

Expanding on the noble gas aspect further, the Warr et al. (2018) study previously demonstrated, that consistent with hydrogeologic models for draining fracture systems, the fluids sampled at 2.4 km showed decreasing mean residence times compared to the samples taken in 2009 (Holland et al., 2013). Although this decrease in residence times is accompanied by reduced radiogenic noble gas concentrations and a modest decrease in salinity (17% and 14.1% for boreholes 12287a and 12,299 respectively), this reduction in fluid residence times had no corresponding effect on the water isotopes (Table 10 - Warr et al., 2018) which remained constant. Likewise, the same study also identified fluids at the deeper level of the mine with an average mean residence time of 1.7 Ga, significantly older than fluids at 2.4 km. Despite this, the isotopic signature for the water remains comparable between the two levels. This indicates that for the given physical parameters (e.g. temperature, water-to-rock ratios etc.) the fluids in the system are also already close to/at isotopic equilibrium with the host rocks and hence the $\delta^{18}O$ and $\delta^{2}H$ values remaining largely constant for the entire Kidd Creek system (always staying within the grey shaded region characteristic of the oldest most saline deep brines; Fig. 2).

### 4.3. A global conceptual model

A conceptual model incorporating the three major controlling processes discussed in this study is presented in Fig. 6.

1. High temperature metamorphic/hydrothermal activity controls the initial isotopic composition of the fluid system either due to hydrothermal components directly or due to high temperature equilibration of other fluids (modified seawater or meteoric water) with the metamorphic/hydrothermal fluids. The immediate precursors to the Precambrian Shield fluids hence likely plot to the right of the GMWL and can be estimated from isotopic studies focusing on metabasalts and metasediments (Taylor, 1974; Sheppard, 1977, 1986).

2. Cooling and mineralisation coupled with long-term, low-temperature equilibration in a low water-rock ratio results in $^{18}O$ depletion in

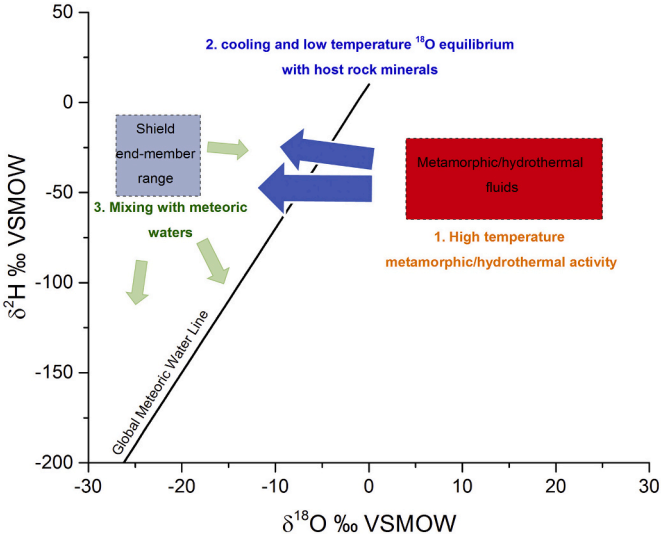


**Fig. 6.** Conceptual model for formation and evolution of saline crystalline basement fluids after Kelly et al. (1986), Guha and Kanwar (1987) and Bottomley et al. (1994) using the metamorphic/hydrothermal fluid range from Kerrich and Ludden (2000) and the range for fracture fluids identified in this work (Fig. 2).

the fracture fluids and the subsequent position of the fluids above/to the left of the GMWL. The long residence times (Ma-Ga) and high salinities of the samples in this study (shaded area Fig. 2) are consistent with the large degree of equilibration required. Some modest degree of $^{2}H$ enrichment may also occur in specific sites due to kaolinite precipitation and/or hydration of feldspars. At this stage the fluids are expected to have developed their characteristic elevated salinities, potentially due to a combination of steps 1 and 2, and/or any site-specific processes.3. Infiltration of meteoric or paleometeoric water occurs through natural and/or anthropogenic activity and resultant mixing with the shield end-members shifts the observed isotopic signatures towards the GMWL. This also results in the salinities of these fluids being diluted as demonstrated in Fig. 4.

An important component of this model are long residence times of the fracture fluids conducive to promoting high degrees of low-temperature isotopic exchange between the fracture fluids and host rocks. For specific sites, additional factors will control locally the exact degree of equilibration ultimately achieved. Variations in both the water-to-rock ratios within the fracture networks and the distribution of $^{18}O$-bearing minerals for instance will play a role in the rate and extent of evolution towards isotopic low-temperature equilibrium between the fracture fluids and the host rock. Considerations of these local factors, coupled with other variables such as geothermal gradients, and/or changes in fracture porosity and geometry alongside the initial fluid origin and composition, the 'precursor' metamorphic fluid isotopic composition, and associated mineral isotopic signatures, and temperature are the primary controls affecting the details of the isotopic signature of these deep crustal fluids on a site specific basis.

The scientific literature on the oxygen and hydrogen isotopic composition of saline fluids from the crystalline basement falling above the GMWL has long struggled with the relative importance of "source" or "precursor" fluid signatures, versus fractionation introduced by alteration during water-rock reactions. To date though there is no clear consensus on the mechanism(s) and relative importance of mechanisms at different sites and while it is widely acknowledged that the trends of co-variation in $\delta^{18}O$ and $\delta^{2}H$ results from both mixing of fluids of different provenance and the effects of water-rock reaction, discussion has nonetheless tended to focus on processes capable of causing fractionation in both oxygen and hydrogen. This paper integrates hundreds of data from sites across three continents and in particular, synthesizes the $\delta^{18}O$ and $\delta^{2}H$ signatures for crystalline fracture fluids from the most hydrogeologically isolated, most saline and oldest systems, of which the Kidd Creek Observatory provides the oldest, with residence times estimated to be more than a billion years. These highly saline Kidd Creek brines, hydrogeologically isolated in the deep subsurface on long geologic timescales (Holland et al., 2013; Warr et al., 2018), have allowed more effective constraints to be placed on the potential end-member composition, permitting deconvolution of the effects of mixing. This study constrains the isotopic characteristics of these end-member fluids more effectively than previous work and demonstrates that investigations into the origin of these crystalline fluid end-members should focus on processes that primarily produce $^{18}O$ fractionation. Building on this insight, a model is developed that can account for these end-member saline fluids at equilibrium with their host rock, based on low-temperature $^{18}O$ equilibration of metamorphic fluids on the long geologic time scales documented for these systems.

## 5. Conclusions

This study presents the first global dataset of water isotope data and salinities compiled from published and unpublished data from S. Africa, Fennoscandia and the Canadian Shield. Careful analysis of this data has allowed differentiation between fluids affected by late-stage mixing with (palaeo)meteoric waters, from fluids with the longest mean residence times that reflect the most saline end-members stored in the host rocks. On a global scale, the most saline Precambrian shield fluids occupy a similar $\delta^{18}O$-$\delta^{2}H$ space considerably more restricted than previously recognised. This suggests a key set of common processes involving metamorphic/hydrothermal fluids and progressive, low temperature $^{18}O/^{16}O$-isotopic equilibration over long geologic timescales control deep crustal fluids dynamics in Precambrian Shield settings globally. Given that 72% of the continental lithosphere by surface area is Precambrian in age (Goodwin, 1996) this finding potentially has implications for modelling the deep hydro(*bio*)geosphere over long geologic timescales and understanding planetary processes relevant to the deep carbon cycle and deep subsurface life. Such insight into major processes controlling subsurface fluids is also relevant to planetary science investigations beyond Earth. For example, the subsurface of Mars is largely tectonically quiescent in the present day with the potential for subsurface fracture networks containing low temperature saline fluids preserved on geologic-planetary timescales (e.g. Michalski et al., 2018, Sherwood Lollar et al., 2007; Tarnas et al., 2018, and references therein).

## Declaration of Competing Interest

The authors declare that they have no known competing financial interests or personal relationships that could have appeared to influence the work reported in this paper.

## Acknowledgements

This study was financially supported by the Canada Research Chairs program, Natural Sciences and Engineering Research Council of Canada Discovery and Accelerator grants, and additional funding was provided by the Deep Carbon Observatory Washington, USA, Nuclear Waste Management Organization and Canadian Institute for Advanced Research (CIFAR) Toronto, Canada. Senior author BSL is a CIFAR Fellow. G. Lollar is thanked for his assistance in compiling the fracture fluid isotopic data. Additional thanks are due to colleagues and supporters at the mines whose efforts and support for the sampling program were invaluable.

## Appendix A. Appendix

**Table A1**
The $\delta^{18}O$ and $\delta^{2}H$ data and accompanying salinities and metadata for 592 fluid samples in this study from fracture networks in Precambrian crystalline rocks compiled from studies from the South African Kaapvaal Craton and the Fennoscandian and Canadian Shields. Where data is from a published source the reference is provided. Samples were collected using three techniques: pumping from boreholes drilled from surface (1); sampling from boreholes drilled from surface by collecting samples at depth with downhole devices (2); or sampling from free-flowing and valved boreholes at depth within mines (3). Sampling methods are provided here as numbers for each sample and are discussed in detail in the main text and references provided.

| Country | Location | Sample ID | Depth (m) | $\partial^{18}O$ | $\partial^{2}H$ | TDS (mg/L) | Source | Sampling Method |
|---|---|---|---|---|---|---|---|---|

(*continued on next page*)

**Table A1** (*continued*)

| Country | Location | Sample ID | Depth (m) | $\partial^{18}O$ | $\partial^{2}H$ | TDS (mg/L) | Source | Sampling Method |
|---|---|---|---|---|---|---|---|---|
| Canada | Birchtree | Bi | nm | −16.3 | −122.0 | nm | Bottomley et al. (1994) | 3 |
| Canada | Birchtree Mine, Thompson | 28.05.2007_BT3950L_BH | 1200 | −14.3 | −69.2 | 114,840 | Unpub. | 3 |
| Canada | Birchtree Mine, Thompson | 28.05.2007_BT3950L_BH1a | 1200 | −15.2 | −74.1 | 105,600 | Unpub. | 3 |
| Canada | Birchtree Mine, Thompson | 29.05.2007_BT3950L_BH3 | 1200 | −14.2 | −64.3 | 118,206 | Unpub. | 3 |
| Canada | Birchtree Mine, Thompson | 06.11.2007_BT_3900_9167N_1113850 | 1190 | −13.6 | −64.2 | 127,710 | Unpub. | 3 |
| Canada | Birchtree Mine, Thompson | 06.11.2007_BT_3900_9167N_1113790 | 1190 | −14.2 | −72.8 | 94,314 | Unpub. | 3 |
| Canada | Birchtree Mine, Thompson | 07.11.2007_BT_3900_9167N_1113860 | 1190 | −14.6 | −74.4 | 99,792 | Unpub. | 3 |
| Canada | Birchtree Mine, Thompson | 08.11.2007_BT_3900_9167N_1113740 | 1190 | −14.4 | −75.6 | 105,864 | Unpub. | 3 |
| Canada | Birchtree Mine, Thompson | 27.03.2008_BT_3950_9167N_BT1 | 1190 | −12.7 | −58.3 | 130,680 | Unpub. | 3 |
| Canada | Campbell | Ca | nm | −12.6 | −91.0 | nm | Bottomley et al. (1994) | 3 |
| Canada | Campbell Mine, Red Lake | Campbell 27–11 | 1220 | −12.2 | −58.2 | 181,744 | Unpub. | 3 |
| Canada | Campbell Mine, Red Lake | Campbell 27–09 | 1220 | −11.5 | −49.3 | 301,535 | Unpub. | 3 |
| Canada | Campbell Mine, Red Lake | Campbell 27–09 | 1220 | −12.0 | −59.2 | 231,428 | Unpub. | 3 |
| Canada | Campbell Mine, Red Lake | Campbell dam | 640 | −13.4 | −105.5 | 783 | Unpub. | 3 |
| Canada | Campbell Mine, Red Lake | Campbell shute | 640 | −13.5 | −106.2 | 715 | Unpub. | 3 |
| Canada | Campbell Mine, Red Lake | Campbell 14–166 | 640 | −14.3 | −110.4 | 2070 | Unpub. | 3 |
| Canada | Campbell Mine, Red Lake | Campbell 14–454 | 640 | −15.1 | −113.4 | 2165 | Unpub. | 3 |
| Canada | CCS | | nm | −12.6 | −84.1 | 31,566 | Unpub. | 3 |
| Canada | CCS | | nm | −12.5 | −84.0 | 30,597 | Unpub. | 3 |
| Canada | CCS | | nm | −12.5 | −94.2 | 3848 | Unpub. | 3 |
| Canada | CCS | | nm | −11.3 | −95.9 | 2906 | Unpub. | 3 |
| Canada | CCS | | nm | −13.2 | −100.5 | 3135 | Unpub. | 3 |
| Canada | CCS | | nm | −11.0 | −58.6 | 83,614 | Unpub. | 3 |
| Canada | CCS | | nm | −11.7 | −64.2 | 77,975 | Unpub. | 3 |
| Canada | CCS | | nm | −11.3 | −47.0 | 127,330 | Unpub. | 3 |
| Canada | CCS | | nm | −11.4 | −47.5 | 102,114 | Unpub. | 3 |
| Canada | Copper Cliff Garson Mine | G-1600 | 1600 | −11.9 | −82.0 | 4279 | Frape and Fritz (1982) | 3 |
| Canada | Copper Cliff North | CC | nm | −13.8 | −94.0 | nm | Bottomley et al. (1994) | 3 |
| Canada | Copper Cliff South Mine | CCS508421 | 500 | −12.2 | −80.0 | 1888 | Frape and Fritz (1982) | 3 |
| Canada | Copper Cliff South Mine | CCS508422 | 500 | −11.7 | −83.0 | 1295 | Frape and Fritz (1982) | 3 |
| Canada | Copper Cliff South Mine | CCS508481 | 500 | −11.8 | −80.0 | 791 | Frape and Fritz (1982) | 3 |
| Canada | Copper Cliff South Mine | CCS205001 | 2050 | −11.4 | −82.0 | 3544 | Frape and Fritz (1982) | 3 |
| Canada | Copper Cliff South Mine | CCS205002 | 2050 | −11.1 | −82.0 | 3989 | Frape and Fritz (1982) | 3 |
| Canada | Copper Cliff South Mine | CCS205003 | 2050 | −11.3 | −98.0 | 3076 | Frape and Fritz (1982) | 3 |
| Canada | Copper Cliff South Mine | CCS3200 | 3200 | −11.1 | −46.0 | 85,789 | Frape and Fritz (1982) | 3 |
| Canada | Copper Cliff South Mine | CCS3250 | 3250 | −10.3 | −44.0 | 94,097 | Frape and Fritz (1982) | 3 |
| Canada | Copper Cliff Wells (Dowling) | 1 | 500 | −13.5 | −89.0 | 220 | Frape and Fritz (1982) | 3 |
| Canada | Copper Cliff Wells (Dowling) | 2 | 500 | −12.9 | −88.0 | 187 | Frape and Fritz (1982) | 3 |
| Canada | Copper Cliff Wells (Dowling) | 3 | 500 | −14.1 | −98.0 | 107 | Frape and Fritz (1982) | 3 |
| Canada | Copper Rand Mine, Chibougaumau | CRV1 | nm | −16.9 | −50.0 | 326,053 | Guha and Kanwar (1987) | 3 |
| Canada | Copper Rand Mine, Chibougaumau | CRV2 | nm | −17.0 | −48.0 | 326,294 | Guha and Kanwar (1987) | 3 |
| Canada | Copper Rand Mine, Chibougaumau | CRV3 | nm | −14.6 | −43.0 | 406,550 | Guha and Kanwar (1987) | 3 |

(*continued on next page*)

**Table A1** (*continued*)

| Country | Location | Sample ID | Depth (m) | $\partial^{18}O$ | $\partial^{2}H$ | TDS (mg/L) | Source | Sampling Method |
|---|---|---|---|---|---|---|---|---|
| Canada | East Bull Lake | P-1 | 32–53.3 | −11.8 | −82.2 | nm | Bottomley et al. (1990) | 1 |
| Canada | East Bull Lake | P-2 | 24.5–38.1 | −11.9 | −86.0 | nm | Bottomley et al. (1990) | 1 |
| Canada | East Bull Lake | P-3 | 0–16 | −11.9 | −85.1 | nm | Bottomley et al. (1990) | 1 |
| Canada | East Bull Lake | P-3 | 16–38.1 | −12.0 | −87.2 | nm | Bottomley et al. (1990) | 1 |
| Canada | East Bull Lake | P-4 | 35–55 | −11.5 | −88.0 | nm | Bottomley et al. (1990) | 1 |
| Canada | East Bull Lake | P-5 | 0–22 | −15.8 | −124.0 | nm | Bottomley et al. (1990) | 1 |
| Canada | East Bull Lake | P-5 | 88.5–97.6 | −17.8 | −136.0 | nm | Bottomley et al. (1990) | 1 |
| Canada | East Bull Lake | P-6 | 0–68 | −11.7 | −80.9 | nm | Bottomley et al. (1990) | 1 |
| Canada | East Bull Lake | P-7 | 0–39.6 | −10.2 | −73.0 | nm | Bottomley et al. (1990) | 1 |
| Canada | East Bull Lake | P-8 | 0–20 | −10.5 | −76.9 | nm | Bottomley et al. (1990) | 1 |
| Canada | East Bull Lake | P-9 | 0–12 | −11.6 | −80.7 | nm | Bottomley et al. (1990) | 1 |
| Canada | East Bull Lake | P-9 | 12–43.2 | −11.6 | −83.9 | nm | Bottomley et al. (1990) | 1 |
| Canada | East Bull Lake | P-10 | 0–34.5 | −11.5 | −79.1 | nm | Bottomley et al. (1990) | 1 |
| Canada | East Bull Lake | P-10 | 34.5–38.5 | −11.3 | −78.5 | nm | Bottomley et al. (1990) | 1 |
| Canada | East Bull Lake | P-10 | 66.3–70.3 | −11.2 | −79.1 | nm | Bottomley et al. (1990) | 1 |
| Canada | East Bull Lake | P-10 | 82–98.7 | −11.2 | −79.8 | nm | Bottomley et al. (1990) | 1 |
| Canada | East Bull Lake | P-11 | 0–49.2 | −11.2 | −81.3 | nm | Bottomley et al. (1990) | 1 |
| Canada | East Bull Lake | P-12 | 0–37 | −11.6 | −80.2 | nm | Bottomley et al. (1990) | 1 |
| Canada | East Bull Lake | P-12 | 38–48.6 | −12.0 | −83.0 | nm | Bottomley et al. (1990) | 1 |
| Canada | East Bull Lake | P-13 | 0–22 | −11.9 | −84.2 | nm | Bottomley et al. (1990) | 1 |
| Canada | East Bull Lake | P-14 | 0–43.3 | −11.8 | −82.6 | nm | Bottomley et al. (1990) | 1 |
| Canada | East Bull Lake | EBL-1 | 147–298 | −13.8 | −111.0 | nm | Bottomley et al. (1990) | 1 |
| Canada | East Bull Lake | EBL-1 | 204–213 | −13.5 | −99.2 | nm | Bottomley et al. (1990) | 1 |
| Canada | East Bull Lake | EBL-1 | 298–512 | −12.4 | −95.0 | nm | Bottomley et al. (1990) | 1 |
| Canada | East Bull Lake | EBL-1 | 504–642 | −13.3 | −95.0 | nm | Bottomley et al. (1990) | 1 |
| Canada | East Bull Lake | EBL-2 | 0–75 | −10.4 | −74.6 | nm | Bottomley et al. (1990) | 1 |
| Canada | East Bull Lake | EBL-2 | 75–248 | −14.1 | −103.4 | nm | Bottomley et al. (1990) | 1 |
| Canada | East Bull Lake | EBL-2 | 111–126 | −16.3 | −120.4 | nm | Bottomley et al. (1990) | 1 |
| Canada | East Bull Lake | EBL-2 | 248–460 | −13.5 | −103.2 | nm | Bottomley et al. (1990) | 1 |
| Canada | East Bull Lake | EBL-2 | 460–616 | −8.7 | −65.4 | nm | Bottomley et al. (1990) | 1 |
| Canada | East Bull Lake | EBL-3 | 0–443 | −11.4 | −79.8 | nm | Bottomley et al. (1990) | 1 |
| Canada | East Bull Lake | EBL-4 | 0–120 | −10.9 | −76.7 | nm | Bottomley et al. (1990) | 1 |
| Canada | East Bull Lake | EBL-4 | 105–117 | −12.9 | −93.9 | nm | Bottomley et al. (1990) | 1 |
| Canada | East Bull Lake | EBL-4 | 120–198 | −15.0 | −104.9 | nm | Bottomley et al. (1990) | 1 |
| Canada | East Bull Lake | EBL-4 | 198–396 | −14.1 | −103.8 | nm | Bottomley et al. (1990) | 1 |
| Canada | East Bull Lake | EBL-4 | 429–456 | −11.9 | −80.3 | nm | Bottomley et al. (1990) | 1 |
| Canada | East Bull Lake | EBL4 | nm | −12.9 | −93.9 | nm | Bottomley et al. (1994) | 1 |
| Canada | Fraser Mine | Fr33170 | 3300 | −12.7 | −78.0 | 21,689 | | 3 |

(*continued on next page*)

**Table A1** (*continued*)

| Country | Location | Sample ID | Depth (m) | $\partial^{18}O$ | $\partial^{2}H$ | TDS (mg/L) | Source | Sampling Method |
|---|---|---|---|---|---|---|---|---|
| | | | | | | | Frape and Fritz (1982) | |
| Canada | Fraser Mine | Fr33182 | 3300 | −12.2 | −70.0 | 29,737 | Frape and Fritz (1982) | 3 |
| Canada | Fraser Mine | Fr33192 | 3300 | −12.8 | −78.0 | 17,713 | Frape and Fritz (1982) | 3 |
| Canada | Fraser Mine | Fr33300 | 3300 | −12.7 | −70.0 | 22,594 | Frape and Fritz (1982) | 3 |
| Canada | Fraser Mine, Sudbury | 08.01.2014_FML4700_FR47774 | 1430 | −11.0 | −33.9 | nm | Unpub. | 3 |
| Canada | Fraser Mine, Sudbury | 06.03.2014_FML4700_FR47774 | 1430 | −10.9 | −33.4 | 39,130 | Unpub. | 3 |
| Canada | Fraser Mine, Sudbury | 06.03.2014_FML4700_FR47774anchor | 1430 | −10.6 | −34.0 | 99,000 | Unpub. | 3 |
| USA | Keweenaw | | nm | −7.6 | −17.1 | 164,395 | Kelly et al. (1986) | 3 |
| USA | Keweenaw | | nm | −7.3 | −25.2 | 204,463 | Kelly et al. (1986) | 3 |
| USA | Keweenaw | | nm | nm | nm | 270,363 | Kelly et al. (1986) | 3 |
| USA | Keweenaw | | nm | nm | −74.0 | 203,550 | Kelly et al. (1986) | 3 |
| Canada | Kidd Creek | KC | nm | −15.5 | −113.0 | nm | Bottomley et al. (1994) | 3 |
| Canada | Kidd Creek Mine, Timmins | 10.05.2007_KC7850_Station_12262 | 2390 | −14.0 | −39.5 | 173,514 | Li et al. (2016) | 3 |
| Canada | Kidd Creek Mine, Timmins | 27.08.2007_KC_7800_Station_12299 | 2390 | −13.1 | −38.5 | 213,105 | Li et al. (2016) | 3 |
| Canada | Kidd Creek Mine, Timmins | 27.08.2007_KC_7800_Station_12287A | 2390 | −12.8 | −38.7 | 175,475 | Li et al. (2016) | 3 |
| Canada | Kidd Creek Mine, Timmins | 27.08.2007_KC_7800_Station_12261 | 2390 | −13.0 | −35.0 | 212,432 | Unpub. | 3 |
| Canada | Kidd Creek Mine, Timmins | 11.02.2008_KC_7800_12299 | 2390 | −12.6 | −36.5 | 175,047 | Unpub. | 3 |
| Canada | Kidd Creek Mine, Timmins | 11.02.2008_KC_7800_12261 | 2390 | −12.8 | −32.0 | nm | Warr et al. (2018) | 3 |
| Canada | Kidd Creek Mine, Timmins | 19.06.2008_KC_7850_12299 | 2390 | −12.8 | −38.6 | 218,170 | Warr et al. (2018) | 3 |
| Canada | Kidd Creek Mine, Timmins | 20.06.2008_KC_785012287A | 2390 | −13.0 | −40.5 | 168,550 | Warr et al. (2018) | 3 |
| Canada | Kidd Creek Mine, Timmins | 31.03.2009_KC_7850_12299 | 2390 | −13.3 | −35.8 | 197,833 | Warr et al. (2018) | 3 |
| Canada | Kidd Creek Mine, Timmins | 12.01.2010_KC_7850_12299 | 2390 | −13.5 | −36.7 | 217,405 | Li et al. (2016) | 3 |
| Canada | Kidd Creek Mine, Timmins | 21.10.2010_KC_7850_12299 | 2390 | −13.6 | −34.2 | 213,759 | Li et al. (2016) | 3 |
| Canada | Kidd Creek Mine, Timmins | 21.10.2010_KC_7850_12287A | 2390 | −13.8 | −36.3 | 167,397 | Li et al. (2016) | 3 |
| Canada | Kidd Creek Mine, Timmins | 21.10.2010_KC_7850_12262 | 2390 | −14.3 | −34.6 | 195,573 | Li et al. (2016) | 3 |
| Canada | Kidd Creek Mine, Timmins | 29.02.2012_KC_7850_12299 | 2390 | −11.6 | −38.0 | 189,117 | Li et al. (2016) | 3 |
| Canada | Kidd Creek Mine, Timmins | 29.02.2012_KC_7850_12287A | 2390 | −12.6 | −38.9 | 135,367 | Unpub. | 3 |
| Canada | Kidd Creek Mine, Timmins | 29.02.2012_KC_7850_12262 | 2390 | −12.1 | −31.7 | 220,357 | Li et al. (2016) | 3 |
| Canada | Kidd Creek Mine, Timmins | 14.06.2012KCL7850_BH12299 | 2390 | −13.4 | −35.7 | 196,612 | Li et al. (2016) | 3 |
| Canada | Kidd Creek Mine, Timmins | 28.11.2012KCL7850_BH12299 | 2390 | −12.4 | −34.7 | 134,087 | Unpub. | 3 |
| Canada | Kidd Creek Mine, Timmins | 28.11.2012KCL7850_BH12287A | 2390 | −12.7 | −34.1 | nm | Unpub. | 3 |
| Canada | Kidd Creek Mine, Timmins | 17.01.2013KCL7850_BH12299 | 2390 | −13.3 | −33.1 | 137,111 | Unpub. | 3 |
| Canada | Kidd Creek Mine, Timmins | 19.09.2013_KC_7850_BH12299 | 2390 | −13.5 | −32.7 | 178,397 | Unpub. | 3 |
| Canada | Kidd Creek Mine, Timmins | 19.09.2013_KC_7850_BH12287A | 2390 | −13.5 | −35.7 | nm | Unpub. | 3 |
| Canada | Kidd Creek Mine, Timmins | 19.09.2013_KC_7850_BH12262 | 2390 | −13.0 | −30.6 | nm | Unpub. | 3 |
| Canada | Kidd Creek Mine, Timmins | 20.09.2013_KC_7850_BH12299 | 2390 | −13.4 | −31.7 | 174,948 | Unpub. | 3 |
| Canada | Kidd Creek Mine, Timmins | 20.09.2013_KC_7850_BH12287A | 2390 | −13.1 | −35.3 | 139,950 | Warr et al. (2018) | 3 |
| Canada | Kidd Creek Mine, Timmins | 02.04.2014_KC_7850_BH12299 | 2390 | −13.0 | −34.4 | 180,473 | Unpub. | 3 |
| Canada | Kidd Creek Mine, Timmins | 02.04.2014_KC_7850_BH12287A | 2390 | −12.6 | −35.8 | 140,748 | Unpub. | 3 |
| Canada | Kidd Creek Mine, Timmins | 02.04.2014_KC_7850_BH12262 | 2390 | −12.9 | −28.6 | 167,329 | Unpub. | 3 |
| Canada | Kidd Creek Mine, Timmins | 03.04.2014_KC_7850_BH12299 | 2390 | −12.9 | −33.1 | 181,307 | Warr et al. (2018) | 3 |

(*continued on next page*)

**Table A1** (*continued*)

| Country | Location | Sample ID | Depth (m) | $\partial^{18}O$ | $\partial^{2}H$ | TDS (mg/L) | Source | Sampling Method |
|---|---|---|---|---|---|---|---|---|
| Canada | Kidd Creek Mine, Timmins | 03.04.2014_KC_7850_BH12262 | 2390 | −12.7 | −29.4 | 165,074 | Unpub. | 3 |
| Canada | Kidd Creek Mine, Timmins | 22.10.2015_KCL7850_BH12299 | 2390 | −11.9 | −36.5 | 141,712 | Unpub. | 3 |
| Canada | Kidd Creek Mine, Timmins | 22.10.2015_KCL7850_BH12262 | 2390 | −11.9 | −33.4 | 170,654 | Unpub. | 3 |
| Canada | Kidd Creek Mine, Timmins | 22.10.2015_KCL7850_BH12287A | 2390 | −12.4 | −35.4 | nm | Unpub. | 3 |
| Canada | Kidd Creek Mine, Timmins | 12.07.2016_KCL7850_BH12299 | 2390 | −12.7 | −34.0 | 177,280 | Lollar et al. (2019) | 3 |
| Canada | Kidd Creek Mine, Timmins | 12.07.2016_KCL7850_BH12261 | 2390 | −12.7 | −33.5 | 203,620 | Lollar et al. (2019) | 3 |
| Canada | Kidd Creek Mine, Timmins | 24.01.2017_KCL7850_BH12299 | 2390 | −12.4 | −34.2 | 168,650 | Unpub. | 3 |
| Canada | Kidd Creek Mine, Timmins | 24.01.2017_KCL7850_BH12261 | 2390 | −12.4 | −33.6 | 205,520 | Unpub. | 3 |
| Canada | Kidd Creek Mine, Timmins | 25.01.2017_KCL7850_BH12287A | 2390 | −12.8 | −38.1 | 137,640 | Unpub. | 3 |
| Canada | Kidd Creek Mine, Timmins | 06.06.2017_KCL7850_BH12299 | 2390 | −11.1 | −34.1 | 172,420 | Unpub. | 3 |
| Canada | Kidd Creek Mine, Timmins | 06.06.2017_KCL7850_BH12261 | 2390 | −11.6 | −33.9 | 192,330 | Unpub. | 3 |
| Canada | Kidd Creek Mine, Timmins | 07.06.2017_KCL7850_BH12287A | 2390 | −10.9 | −35.4 | 147,880 | Unpub. | 3 |
| Canada | Kidd Creek Mine, Timmins | 29.01.2018_KCL7850_BH12299 | 2390 | −12.4 | −35.5 | 179,800 | Unpub. | 3 |
| Canada | Kidd Creek Mine, Timmins | 14.6.2018-KC7850–12299 | 2390 | −12.6 | −38.0 | 189,220 | Unpub. | 3 |
| Canada | Kidd Creek Mine, Timmins | 14.6.2018-KC7850–12261 | 2390 | −12.7 | −35.4 | 206,700 | Unpub. | 3 |
| Canada | Kidd Creek Mine, Timmins | 05.02.2019_KC7850_12299 | 2390 | −13.1 | −33.9 | 186,570 | Unpub. | 3 |
| Canada | Kidd Creek Mine, Timmins | 05.02.2019_KC7850_12261 | 2390 | −13.0 | −33.0 | 216,290 | Unpub. | 3 |
| Canada | Kidd Creek Mine, Timmins | 10.05.06_KC_8798_980R_11404 | 2680 | −12.0 | −59.3 | 134,109 | Unpub. | 3 |
| Canada | Kidd Creek Mine, Timmins | 01.04.2009_KC_9500_12612A | 2740 | −9.0 | −86.8 | 1449 | Unpub. | 3 |
| Canada | Kidd Creek Mine, Timmins | 29.02.2012_KC_9500_13677 | 2900 | −10.1 | −81.0 | 3335 | Unpub. | 3 |
| Canada | Kidd Creek Mine, Timmins | 14.06.2012KCL9500_BH13684 | 2900 | −17.5 | −30.9 | 209,042 | Unpub. | 3 |
| Canada | Kidd Creek Mine, Timmins | 14.06.2012KCL9500_BH13762 | 2900 | −16.6 | −29.3 | 215,148 | Unpub. | 3 |
| Canada | Kidd Creek Mine, Timmins | 29.11.2012KCL9500_BH13762 | 2900 | −9.4 | −73.8 | 7527 | Unpub. | 3 |
| Canada | Kidd Creek Mine, Timmins | 16.01.2013KCL9500_BH13762 | 2900 | −9.7 | −77.3 | 2737 | Unpub. | 3 |
| Canada | Kidd Creek Mine, Timmins | 16.01.2013KCL9500_BH2 | 2900 | −13.8 | −28.4 | nm | Unpub. | 3 |
| Canada | Kidd Creek Mine, Timmins | 16.01.2013KCL9500_BH4 | 2900 | −11.9 | −49.3 | nm | Unpub. | 3 |
| Canada | Kidd Creek Mine, Timmins | 17.01.2013KCL9200_BH1 | 2805 | −9.5 | −76.5 | 4415 | Unpub. | 3 |
| Canada | Kidd Creek Mine, Timmins | 17.01.2013KCL9200_BH2 | 2805 | −7.9 | −69.2 | nm | Unpub. | 3 |
| Canada | Kidd Creek Mine, Timmins | 26.09.2013_KC_9500_BH13879 | 2900 | −11.8 | −52.8 | nm | Unpub. | 3 |
| Canada | Lockerby Mine | L40139 | 4000 | −11.7 | −84.0 | 4538 | Frape and Fritz (1982) | 3 |
| Canada | Lockerby Mine | L40140 | 4000 | −12.1 | −79.0 | 23,170 | Frape and Fritz (1982) | 3 |
| Canada | Lockerby Mine | L40141 | 4000 | −11.6 | −80.0 | 6862 | Frape and Fritz (1982) | 3 |
| Canada | Lockerby Mine | L40143 | 4000 | −11.7 | −80.0 | 13,128 | Frape and Fritz (1982) | 3 |
| Canada | Lockerby Mine | L26000 | 2600 | −11.5 | −85.0 | 128 | Frape and Fritz (1982) | 3 |
| Canada | Lockerby Mine | L261350 | 2600 | −12.8 | −92.0 | 1964 | Frape and Fritz (1982) | 3 |
| Canada | Lockerby Mine | L261400 | 2600 | nm | nm | nm | Frape and Fritz (1982) | 3 |
| Canada | Lockerby Mine | L261450 | 2600 | −11.2 | −86.0 | 2596 | Frape and Fritz (1982) | 3 |
| Canada | Lockerby Mine | L261650 | 2600 | −11.6 | −92.0 | 1061 | | 3 |

(*continued on next page*)

**Table A1** (*continued*)

| Country | Location | Sample ID | Depth (m) | $\partial^{18}O$ | $\partial^{2}H$ | TDS (mg/L) | Source | Sampling Method |
|---|---|---|---|---|---|---|---|---|
| | | | | | | | Frape and Fritz (1982) | |
| Canada | Lockerby Mine | L261750 | 2600 | −11.7 | −80.0 | nm | Frape and Fritz (1982) | 3 |
| Canada | Lockerby Mine | L22450 | 2600 | nm | −81.0 | 1282 | Frape and Fritz (1982) | 3 |
| Canada | Lupin Mine | BH 188 | 890 | −22.4 | −178.0 | 3600 | Stotler et al. (2009) | 3 |
| Canada | Lupin Mine | BH 188 | 890 | −22.1 | −175.0 | 2800 | Stotler et al. (2009) | 3 |
| Canada | Lupin Mine | BH 188 | 890 | −22.4 | −180.0 | 3100 | Stotler et al. (2009) | 3 |
| Canada | Lupin Mine | BH 188, pressurized | 890 | −22.8 | −176.0 | 3000 | Stotler et al. (2009) | 3 |
| Canada | Lupin Mine | BH 188, pressurized | 890 | −22.9 | −179.0 | 2700 | Stotler et al. (2009) | 3 |
| Canada | Lupin Mine | BH 188, pressurized | 890 | −22.5 | −182.0 | 3200 | Stotler et al. (2009) | 3 |
| Canada | Lupin Mine | BH 188, pressurized | 890 | −22.8 | −178.0 | 2800 | Stotler et al. (2009) | 3 |
| Canada | Lupin Mine | BH 188, pressurized | 890 | −22.7 | −179.0 | 2800 | Stotler et al. (2009) | 3 |
| Canada | Lupin Mine | BH 64 | 1130 | −23.3 | −181.0 | 2200 | Stotler et al. (2009) | 3 |
| Canada | Lupin Mine | BH 64 | 1130 | −23.0 | −184.0 | 2800 | Stotler et al. (2009) | 3 |
| Canada | Lupin Mine | BH 64 | 1130 | −23.4 | −181.0 | 2600 | Stotler et al. (2009) | 3 |
| Canada | Lupin Mine | BH 64 | 1130 | −23.3 | −182.0 | nm | Stotler et al. (2009) | 3 |
| Canada | Lupin Mine | BH 175, flowing | 1130 | −22.6 | −177.0 | 26,200 | Stotler et al. (2009) | 3 |
| Canada | Lupin Mine | BH 175, flowing | 1130 | −22.8 | −174.0 | 27,500 | Stotler et al. (2009) | 3 |
| Canada | Lupin Mine | BH 175, flowing | 1130 | −22.5 | −173.0 | 32,100 | Stotler et al. (2009) | 3 |
| Canada | Lupin Mine | BH 191 | 1130 | −23.2 | −179.0 | 7100 | Stotler et al. (2009) | 3 |
| Canada | Lupin Mine | BH 191 | 1130 | −23.2 | −179.0 | 7700 | Stotler et al. (2009) | 3 |
| Canada | Lupin Mine | BH 191, pressurized | 1130 | −23.4 | −180.0 | 5800 | Stotler et al. (2009) | 3 |
| Canada | Lupin Mine | BH 191, pressurized | 1130 | −23.0 | −179.0 | 13,700 | Stotler et al. (2009) | 3 |
| Canada | Lupin Mine | BH 191, pressurized | 1130 | −23.0 | −182.0 | 7000 | Stotler et al. (2009) | 3 |
| Canada | Lupin Mine | BH 192 | 1130 | −22.6 | −181.0 | 30,700 | Stotler et al. (2009) | 3 |
| Canada | Lupin Mine | BH 192 | 1130 | −22.8 | −175.0 | 29,700 | Stotler et al. (2009) | 3 |
| Canada | Lupin Mine | BH 192, pressurized | 1130 | −22.7 | −175.0 | 36,300 | Stotler et al. (2009) | 3 |
| Canada | Lupin Mine | BH 192, pressurized | 1130 | −22.2 | −176.0 | 40,000 | Stotler et al. (2009) | 3 |
| Canada | Lupin Mine | BH 192, pressurized | 1130 | −22.5 | −172.0 | 39,900 | Stotler et al. (2009) | 3 |
| Canada | Lupin Mine | BH 192, pressurized | 1130 | −22.6 | −173.0 | 39,600 | Stotler et al. (2009) | 3 |
| Canada | Lupin Mine | BH 197 | 1130 | −22.8 | −186.0 | 9100 | Stotler et al. (2009) | 3 |
| Canada | Lupin Mine | BH 197, pressurized | 1130 | −23.0 | −178.0 | 8600 | Stotler et al. (2009) | 3 |
| Canada | Lupin Mine | BH 197, pressurized | 1130 | −22.9 | −179.0 | 5900 | Stotler et al. (2009) | 3 |
| Canada | Lupin Mine | BH 197, pressurized | 1130 | −22.4 | −180.0 | 9600 | Stotler et al. (2009) | 3 |
| Canada | Lupin Mine | BH 197, pressurized | 1130 | −22.8 | −178.0 | 6400 | Stotler et al. (2009) | 3 |
| Canada | Lupin Mine | BH 197, pressurized | 1130 | −22.7 | −179.0 | 5900 | Stotler et al. (2009) | 3 |
| Canada | Lupin Mine | BH 217, pressurized | 1130 | −23.5 | −179.0 | 8500 | Stotler et al. (2009) | 3 |
| Canada | Lupin Mine | BH 217, pressurized | 1130 | −23.2 | −180.0 | 15,500 | Stotler et al. (2009) | 3 |
| Canada | Lupin Mine | BH 217, pressurized | 1130 | −22.9 | −182.0 | 7000 | Stotler et al. (2009) | 3 |
| Canada | Lupin Mine | BH 217, pressurized | 1130 | −23.1 | −179.0 | 13,200 | Stotler et al. (2009) | 3 |
| Canada | Lupin Mine | BH 219, pressurized | 1130 | −23.0 | −179.0 | 10,100 | Stotler et al. (2009) | 3 |
| Canada | Lupin Mine | BH 219, pressurized | 1130 | −22.9 | −179.0 | 20,600 | Stotler et al. (2009) | 3 |
| Canada | Lupin Mine | BH 219, pressurized | 1130 | −22.9 | −178.0 | 8100 | Stotler et al. (2009) | 3 |
| Canada | Lupin Mine | BH 260 | 1130 | −23.0 | −177.0 | 15,900 | Stotler et al. (2009) | 3 |
| Canada | Lupin Mine | BH 260 | 1130 | −23.0 | −183.0 | 8800 | Stotler et al. (2009) | 3 |
| Canada | Lupin Mine | BH 260 | 1130 | −23.1 | −179.0 | 12,100 | Stotler et al. (2009) | 3 |
| Canada | Lupin Mine | BH 267, 3–24 m | 1130 | −23.1 | −185.0 | 4100 | Stotler et al. (2009) | 3 |
| Canada | Lupin Mine | BH 267, 45–66 m | 1130 | −23.1 | −186.0 | 4700 | Stotler et al. (2009) | 3 |
| Canada | Lupin Mine | BH 267, 187–269 m | 1130 | −23.0 | −185.0 | 5600 | Stotler et al. (2009) | 3 |
| Canada | Lupin Mine | BH 267, pressurized | 1130 | −23.4 | −180.0 | 6100 | Stotler et al. (2009) | 3 |
| Canada | Lupin Mine | BH 267, leaking | 1130 | −23.2 | −183.0 | 4800 | Stotler et al. (2009) | 3 |
| Canada | Lupin Mine | BH 273, pressurized | 1130 | −22.8 | −182.0 | 11,900 | Stotler et al. (2009) | 3 |
| Canada | Lupin Mine | BH 273, pressurized | 1130 | −23.2 | −178.0 | 7900 | Stotler et al. (2009) | 3 |
| Canada | Lupin Mine | BH 273, pressurized | 1130 | −23.2 | −179.0 | 10,200 | Stotler et al. (2009) | 3 |
| Canada | Lupin Mine | BH 273, pressurized | 1130 | −23.0 | −180.0 | 8300 | Stotler et al. (2009) | 3 |
| Canada | Lupin Mine | Drips, Bolthole | 1130 | −23.4 | −180.0 | 3900 | Stotler et al. (2009) | 3 |
| Canada | Lupin Mine | Drips, Bolthole | 1130 | −22.9 | −184.0 | 4100 | Stotler et al. (2009) | 3 |
| Canada | Lupin Mine | BH 105 | 1300 | −22.8 | −180.0 | 9100 | Stotler et al. (2009) | 3 |
| Canada | Lupin Mine | Purge 1 | 535 | −17.7 | −147.0 | 107,187 | Stotler et al. (2011) | 2 |
| Canada | Lupin Mine | Purge 4 | 535 | −22.2 | −175.0 | 29,735 | Stotler et al. (2011) | 2 |
| Canada | Lupin Mine | Purge 6 | 535 | −22.5 | −177.0 | 22,077 | Stotler et al. (2011) | 2 |
| Canada | Lupin Mine | Purge 7 | 535 | −22.6 | −177.0 | 21,240 | Stotler et al. (2011) | 2 |
| Canada | Lupin Mine | Lu | nm | −21.3 | −167.0 | 12,469 | Bottomley et al. (1994) | 3 |
| Canada | Matagami | R28 | 0 | −13.9 | −107.0 | 26,692 | Unpub. | 3 |
| Canada | Matagami | R36 | 0 | −11.5 | −60.8 | 223,635 | Unpub. | 3 |
| Canada | Matagami | −25 | 360 | −14.1 | −95.9 | 752 | Unpub. | 3 |
| Canada | Matagami | −25’ | 360 | −14.4 | −107.5 | 386 | Unpub. | 3 |
| Canada | Matagami | −35 | 360 | −14.1 | −85.6 | 1329 | Unpub. | 3 |
| Canada | Matagami | Wall | 360 | −14.5 | −105.0 | 1035 | Unpub. | 3 |
| Canada | Matagami | Drip #1 | 610 | −14.4 | −98.8 | 458 | Unpub. | 3 |
| Canada | Nickel Rim South Mine, Sudbury | 29.11.2013_NR_1730m_NR170128 | 1730 | −11.9 | −30.9 | 47,645 | Unpub. | 3 |

(*continued on next page*)

**Table A1** (*continued*)

| Country | Location | Sample ID | Depth (m) | $\partial^{18}O$ | $\partial^{2}H$ | TDS (mg/L) | Source | Sampling Method |
|---|---|---|---|---|---|---|---|---|
| Canada | Nickel Rim South Mine, Sudbury | 29.11.2013_NR_550SumpStation_NR170155 | 1730 | −11.4 | −31.9 | 42,055 | Unpub. | 3 |
| Canada | Nickel Rim South Mine, Sudbury | 05.03.2014_NR_1730m_NR170128 | 1730 | −11.5 | −30.3 | 53,365 | Unpub. | 3 |
| Canada | Nickel Rim South Mine, Sudbury | 22.10.2014_NR_1730m_NR170128 | 1730 | −13.0 | −35.6 | 71,412 | Unpub. | 3 |
| Canada | Nickel Rim South Mine, Sudbury | 22.10.2014_NR_1730m_NR170183 | 1730 | −12.1 | −30.2 | nm | Unpub. | 3 |
| Canada | Nickel Rim South Mine, Sudbury | 22.10.2014_NR_1730m_NR170185 | 1730 | −12.2 | −30.2 | 98,934 | Unpub. | 3 |
| Canada | Nickel Rim South Mine, Sudbury | 22.10.2014_NR_1730m_NR170215 | 1730 | −11.0 | −46.7 | 37,960 | Unpub. | 3 |
| Canada | Nickel Rim South Mine, Sudbury | 22.10.2014_NR_1730m_NR170216 | 1730 | −11.1 | −48.9 | 26,585 | Unpub. | 3 |
| Canada | Norita | | nm | −14.0 | −99.6 | 14,756 | Unpub. | 3 |
| Canada | Norita | | nm | −13.8 | −90.0 | 105,320 | Unpub. | 3 |
| Canada | Norita | | 61 | −13.5 | −92.5 | 121,829 | Unpub. | 3 |
| Canada | Norita | | 76 | −13.7 | −85.5 | 128,469 | Unpub. | 3 |
| Canada | Norita | | 91 | −13.5 | −89.4 | 141,184 | Unpub. | 3 |
| Canada | Norita | | 230 | −13.2 | −70.0 | 213,644 | Unpub. | 3 |
| Canada | Norita | | 244 | −13.4 | −70.8 | 217,951 | Unpub. | 3 |
| Canada | North Mine | N3601 | 3600 | −13.0 | −88.0 | 5303 | Frape and Fritz (1982) | 3 |
| Canada | North Mine | N3602 | 3600 | −13.1 | −88.0 | 6290 | Frape and Fritz (1982) | 3 |
| Canada | North Mine | N3640 | 3600 | −11.0 | −40.0 | 225,446 | Frape and Fritz (1982) | 3 |
| Canada | North Mine | N3643 | 3600 | −13.4 | −94.0 | 4113 | Frape and Fritz (1982) | 3 |
| Canada | North Mine | N3644 | 3600 | −12.0 | −83.0 | 264 | Frape and Fritz (1982) | 3 |
| Canada | North Mine | N3651 | 3600 | −11.3 | −33.0 | 240,632 | Frape and Fritz (1982) | 3 |
| Canada | Red Lake, ON, Campbell Mine | | 1220 | −12.2 | −58.2 | 181,744 | Unpub. | 3 |
| Canada | Red Lake, ON, Campbell Mine | | 1220 | −11.5 | −49.3 | 301,535 | Unpub. | 3 |
| Canada | Red Lake, ON, Campbell Mine | | 1220 | −12.0 | −59.2 | 231,428 | Unpub. | 3 |
| Canada | Red Lake, ON, Campbell Mine | | 640 | −13.4 | −105.5 | 783 | Unpub. | 3 |
| Canada | Red Lake, ON, Campbell Mine | | 640 | −13.5 | −106.2 | 715 | Unpub. | 3 |
| Canada | Red Lake, ON, Campbell Mine | | 640 | −14.3 | −110.4 | 2070 | Unpub. | 3 |
| Canada | Red Lake, ON, Campbell Mine | | 640 | −15.1 | −113.4 | 2165 | Unpub. | 3 |
| Canada | Sudbury | S-138 | 1600 | −10.9 | −44.0 | 252,000 | Frape et al. (1984) | 3 |
| Canada | Sudbury | S-139 | 1600 | −10.3 | −42.0 | 240,000 | Frape et al. (1984) | 3 |
| Canada | Sudbury | S-144 | 1650 | −10.8 | −45.0 | 254,000 | Frape et al. (1984) | 3 |
| Canada | Sudbury | S-147 | 1600 | −10.9 | −39.0 | 249,121 | Frape et al. (1984) | 3 |
| Canada | Sudbury | S-149 | 1600 | −11.3 | −33.0 | 240,632 | Frape et al. (1984) | 3 |
| Canada | Sudbury | S-176 | 488 | −11.9 | −82.0 | 4278 | Frape et al. (1984) | 3 |
| Canada | Sudbury | S-160 | 50 | −11.5 | −85.0 | 127 | Frape et al. (1984) | 3 |
| Canada | Sudbury | S-178 | 152 | −12.9 | −88.0 | 186 | Frape et al. (1984) | 3 |
| Canada | Sudbury | S-145 | 1100 | −11.9 | −73.0 | 83,373 | Frape et al. (1984) | 3 |
| Canada | Sudbury | S-154 | 1006 | −12.8 | −76.0 | 18,812 | Frape et al. (1984) | 3 |
| Canada | Sudbury | S-175 | 991 | −10.4 | −43.0 | 95,039 | Frape et al. (1984) | 3 |
| Canada | Sudbury | | nm | −11.3 | −33.0 | 240,632 | Kelly et al. (1986) | 3 |
| Canada | Thompson | T-93 | 1500 | −11.7 | −53.0 | 325,000 | Frape et al. (1984) | 3 |
| Canada | Thompson | T-94 | 1220 | −14.4 | −79.0 | 182,600 | Frape et al. (1984) | 3 |
| Canada | Thompson | T-95 | 1220 | −15.6 | −92.0 | 101,433 | Frape et al. (1984) | 3 |
| Canada | Thompson | T-97 | 1300 | −13.2 | −77.0 | 117,292 | Frape et al. (1984) | 3 |
| Canada | Thompson | T-86 | 610 | −17.9 | −127.0 | 20,338 | Frape et al. (1984) | 3 |
| Canada | Thompson | T-87 | 671 | −17.0 | −115.0 | 22,495 | Frape et al. (1984) | 3 |
| Canada | Thompson | T-92 | 1220 | −16.0 | −102.0 | 65,437 | Frape et al. (1984) | 3 |
| Canada | Thompson | T-82 | 305 | −16.3 | −128.0 | 1798 | Frape et al. (1984) | 3 |
| Canada | Thompson | T-83 | 305 | −17.4 | −131.0 | 5371 | Frape et al. (1984) | 3 |
| Canada | Thompson | T-79 | 100 | −18.9 | −149.0 | 580 | Frape et al. (1984) | 3 |
| Canada | Thompson | T-80 | 152 | −18.1 | −137.0 | 589 | Frape et al. (1984) | 3 |
| Canada | Thompson | T-96 | 50 | −13.7 | −115.0 | 117 | Frape et al. (1984) | 3 |
| Canada | Thompson Mine, Thompson | 12.10.2006_TH3600L_Sta7_"BH#7" | 1200 | −13.0 | −64.8 | nm | Unpub. | 3 |
| Canada | Thompson Mine, Thompson | 12.10.2006_TH3600L_Sta7_"BH#4" | 1200 | −14.3 | −81.0 | 156,417 | Unpub. | 3 |
| Canada | Thompson Mine, Thompson | 12.10.2006_TH3600L_Sta7_"BH#1" | 1200 | −14.6 | −80.2 | 203,508 | Unpub. | 3 |
| Canada | Thompson Mine, Thompson | 11.10.2006_TH3500L_Sta389_BH106583 | 1200 | −15.0 | −97.4 | nm | Unpub. | 3 |
| Canada | Thompson Mine, Thompson | 11.10.2006_TH3500L_Sta390 | 1200 | −14.5 | −85.7 | nm | Unpub. | 3 |
| Canada | | 11.10.2006_TH3500L_Sta396 | 1200 | −14.7 | −85.6 | nm | Unpub. | 3 |

(*continued on next page*)

**Table A1** (*continued*)

| Country | Location | Sample ID | Depth (m) | $\partial^{18}O$ | $\partial^{2}H$ | TDS (mg/L) | Source | Sampling Method |
|---|---|---|---|---|---|---|---|---|
| | Thompson Mine, Thompson | | | | | | | |
| Canada | Thompson Mine, Thompson | 11.10.2006_TH3500L_Sta396_BH116385 | 1200 | −17.3 | −91.1 | nm | Unpub. | 3 |
| Canada | Thompson Mine, Thompson | 11.10.2006_TH3500L_Sta392 | 1200 | −14.7 | −90.7 | nm | Unpub. | 3 |
| Canada | Thompson Mine, Thompson | 11.10.2006_TH3500L_Sta396_BH106547 | 1200 | −13.6 | −92.8 | nm | Unpub. | 3 |
| Canada | Thompson Mine, Thompson | 11.10.2006_TH3500L_Sta391 | 1200 | −14.6 | −85.6 | nm | Unpub. | 3 |
| Canada | Thompson Mine, Thompson | 11.10.2006_TH3500L_Sta396_BH116386 | 1200 | −16.1 | −99.4 | nm | Unpub. | 3 |
| Canada | Thompson Mine, Thompson | 11.10.2006_TH3500L_Sta390_BH116392 | 1200 | −14.8 | −85.7 | 157,753 | Unpub. | 3 |
| Canada | Thompson Mine, Thompson | 1163630 13.06.06 | 1200 | −13.3 | −97.4 | 39,692 | Telling et al. (2018) | 3 |
| Canada | Thompson Mine, Thompson | 1065750 13.06.06 | 1200 | −14.7 | −82.8 | 204,755 | Telling et al. (2018) | 3 |
| Canada | Thompson Mine, Thompson | 1065800 13.06.06 | 1200 | −13.3 | −104.2 | nm | Telling et al. (2018) | 3 |
| Canada | Thompson Mine, Thompson | 1065760 14.06.06 | 1200 | −14.5 | −94.8 | nm | Telling et al., 2018 | 3 |
| Canada | Thompson Mine, Thompson | 1163930 14.06.06 | 1200 | −15.3 | −98.5 | 83,452 | Telling et al. (2018) | 3 |
| Canada | Thompson No. 1 Shaft | T1 | nm | −13.4 | −94.0 | nm | Bottomley et al. (1994) | 3 |
| Canada | Thompson No. 3 Shaft | T3 | nm | −15.5 | −106.0 | nm | Bottomley et al. (1994) | 3 |
| Canada | Thompson | 777 m: no # (10/97) | 777 | −12.4 | −111 | 367 | Bottomley and Clark (2004) | 3 |
| Canada | Victor Mine | 1463 m: B-99162 (03/98) | 1463 | −11.7 | −31 | 98,790 | Bottomley and Clark (2004) | 3 |
| Canada | Victor Mine | 1463 m: B-99160 (03/98) | 1463 | −11.7 | −32 | 113,309 | Bottomley and Clark (2004) | 3 |
| Canada | Yellowknife | YK-62 | 130 | −19.6 | −161.0 | 850 | Frape et al. (1984) | 3 |
| Canada | Yellowknife | YK-65 | 175 | −19.7 | −153.0 | 740 | Frape et al. (1984) | 3 |
| Canada | Yellowknife | YK-17 | 1500 | −14.4 | −71.0 | 237,107 | Frape et al. (1984) | 3 |
| Canada | Yellowknife | YK-15 | 1372 | −19.1 | −123.0 | 108,799 | Frape et al. (1984) | 3 |
| Canada | Yellowknife | YK-32 | 1372 | −16.9 | −91.0 | 193,000 | Frape et al. (1984) | 3 |
| Canada | Yellowknife | YK-33 | 1372 | −18.1 | −105.0 | 172,900 | Frape et al. (1984) | 3 |
| Canada | Yellowknife | YK-34 | 550 | −20.4 | −162.0 | 1770 | Frape et al. (1984) | 3 |
| Canada | Yellowknife | YK-71 | 335 | −19.2 | −163.0 | 4223 | Frape et al. (1984) | 3 |
| Canada | Yellowknife | YK-73 | 457 | −19.1 | −152.0 | 8831 | Frape et al. (1984) | 3 |
| Canada | Yellowknife | YK-9 | 1372 | −19.9 | −145.0 | 58,337 | Frape et al. (1984) | 3 |
| Canada | Yellowknife | YK-10 | 1372 | −23.0 | −163.0 | 63,136 | Frape et al. (1984) | 3 |
| Canada | Yellowknife | YK-22 | 1494 | −19.1 | −140.0 | 20,481 | Frape et al. (1984) | 3 |
| Canada | Yellowknife | | nm | −14.4 | −73.0 | 261,478 | Kelly et al. (1986) | 3 |
| Canada | Yellowknife | 1067 m: seep (02/95) | 1067 | −19.3 | −157 | 336.6 | Bottomley and Clark (2004) | 3 |
| Canada | Yellowknife | 1067 m: B-8906 (09/00) | 1067 | −19.4 | −154 | 538.6 | Bottomley and Clark (2004) | 3 |
| Canada | Yellowknife | 1067 m: B-9452 (09/00) | 1067 | −19.8 | −157 | 4105.5 | Bottomley and Clark (2004) | 3 |
| Canada | Yellowknife | 1067 m: B-9362 (09/00) | 1067 | −20.9 | −162 | 5725.6 | Bottomley and Clark (2004) | 3 |
| Canada | Yellowknife | 1372 m: B-3457 (02/95) | 1372 | −20.4 | −161 | 10,086.6 | Bottomley and Clark (2004) | 3 |
| Canada | Yellowknife | 1372 m: B-5316 (09/00) | 1372 | −20.4 | −161 | 11,534.5 | Bottomley and Clark (2004) | 3 |
| Canada | Yellowknife | 1372 m: B-5318 (09/00) | 1372 | −19.2 | −150 | 30,202.4 | Bottomley and Clark (2004) | 3 |
| Canada | Yellowknife | 1372 m: B-3316 (02/95) | 1372 | −17.2 | −103 | 106,202.5 | Bottomley and Clark (2004) | 3 |
| Canada | Yellowknife | 1494 m: B-5310 (09/00) | 1494 | −19.4 | −134 | 70,499.2 | Bottomley and Clark (2004) | 3 |
| Canada | Yellowknife | 1494 m: seep (02/95) | 1494 | −17.6 | −111 | 102,588.4 | Bottomley and Clark (2004) | 3 |
| Canada | Yellowknife | 1616 m: B-7126 (09/00) | 1616 | −13.6 | −73 | 165,114.7 | Bottomley and Clark (2004) | 3 |
| Canada | Yellowknife | 1616 m: B-6790 (09/00) | 1616 | −14.3 | −73 | 170,969.3 | Bottomley and Clark (2004) | 3 |
| Canada | Yellowknife | 1616 m: B-5586 (06/96) | 1616 | −14.4 | −69 | 175,933.7 | Bottomley and Clark (2004) | 3 |
| Canada | Yellowknife | 1616 m: B-6709 (06/96) | 1616 | −13.6 | −62 | 190,390.7 | Bottomley and Clark (2004) | 3 |

(*continued on next page*)

**Table A1** (*continued*)

| Country | Location | Sample ID | Depth (m) | $\partial^{18}O$ | $\partial^{2}H$ | TDS (mg/L) | Source | Sampling Method |
|---|---|---|---|---|---|---|---|---|
| S. Africa | Beatrix | BE224 FW 032601C18W17 | 768.0 | −6.13 | −42.7 | 2276 | Lippmann et al. (2003) | 3 |
| S. Africa | Beatrix | BE325 H1 032701 CTS | 1290.0 | −6.71 | −43.2 | 2424 | Lippmann et al. (2003) | 3 |
| S. Africa | Beatrix | BE327 H3 032701 CTS | 1390.0 | −6.66 | −41.2 | 2772 | Lippmann et al. (2003) | 3 |
| S. Africa | Beatrix | BE116 H1 031601 GDW | 866.0 | −5.85 | −42.33 | 2012 | Lippmann et al. (2003) | 3 |
| S. Africa | Beatrix | BE116 FW 031401 IDW | 866.0 | −5.49 | −40.1 | 2244 | Lippmann et al. (2003) | 3 |
| S. Africa | Beatrix | BE23FW-A4RD | 718.0 | −6.2 | −41.0 | nm | Lippmann et al. (2003) | 3 |
| S. Africa | Beatrix | BE116 FW 121801 | 866.0 | −6.86 | −40.7 | 2015 | Onstott et al. (2006) | 3 |
| S. Africa | Beatrix | BE116 GS 031401 EDW | 866.0 | −6.00 | −41.5 | 1262 | Onstott et al. (2006) | 3 |
| S. Africa | Beatrix | BE116 H2 031601 GDW | 866.0 | −4.46 | −39.9 | nm | Onstott et al. (2006) | 3 |
| S. Africa | Beatrix | BE116 H3 031601 GDW | 866.0 | −6.24 | −40:9 | nm | Onstott et al. (2006) | 3 |
| S. Africa | Beatrix | BE223 FW 031301 A4RD | 718.0 | −6.37 | −39.7 | nm | Onstott et al. (2006) | 3 |
| S. Africa | Beatrix | BE324 FW 121801 | 1240.0 | −6.88 | −41.0 | 2428 | Onstott et al. (2006) | 3 |
| S. Africa | Beatrix | BE326 Bh2 2011 | 1330.0 | −5.9 | −41.0 | 4470 | Lau et al. (2014) | 3 |
| S. Africa | Beatrix | BE326 Bh2 2012 | 1330.0 | −8.7 | −47.0 | nm | Lau et al. (2014) | 3 |
| S. Africa | Beatrix | BE326 Bh2 2012 | 1330.0 | −6.4 | −41.4 | 3590 | Simkus et al. (2016) | 3 |
| S. Africa | Beatrix | BE326 Bh1 | 1330.0 | −6.6 | −41.7 | 3410 | Simkus et al. 2016 | 3 |
| S. Africa | Driefontein | DR546 BH1 120798 | 3213.0 | −13.14 | −24.4 | 35,041 | Lippmann et al. (2003) | 3 |
| S. Africa | Driefontein | DR4 IPC H1 090198 | 945.0 | −4.55 | −20.3 | 238 | Onstott et al. (2006) | 3 |
| S. Africa | Driefontein | DR4 IPC HI 082902 | 945.0 | −3.58 | −18.0 | 176 | Onstott et al. (2006) | 3 |
| S. Africa | Driefontein | DR548 FW 090901 | 3300.0 | −12.29 | −10.3 | 101,074 | Onstott et al. (2006) | 3 |
| S. Africa | Driefontein | DR638 FW 111598 | 2700.0 | −6.20 | −34.0 | 885 | Onstott et al. (2006) | 3 |
| S. Africa | Driefontein | DR938 H1 082001 | 2716.0 | −4.31 | −26.7 | 211 | Onstott et al. (2006) | 3 |
| S. Africa | Driefontein | DR938 H3 083001 | 2716.0 | −5.01 | −27.9 | 1826 | Onstott et al. (2006) | 3 |
| S. Africa | Driefontein | DR938 H3 071202 | 3350.0 | −5.64 | −26.9 | 1696 | Onstott et al. (2006) | 3 |
| S. Africa | Driefontein | DR938 H3 082802 | 2712.0 | −5.80 | −27.7 | 1687 | Onstott et al. (2006) | 3 |
| S. Africa | Driefontein | DR938 H4 110201 | 2176.0 | −4.68 | −26.3 | 127 | Onstott et al. (2006) | 3 |
| S. Africa | Driefontein | DR940 FW 092602 | 2812.0 | −4.78 | −27.2 | 264 | Onstott et al. (2006) | 3 |
| S. Africa | Driefontein | DR5IPCFW280711 | 1046.0 | −4.3 | −24.6 | nm | Lau et al. (2014) | 3 |
| S. Africa | Driefontein | DR5IPC | 1050.0 | −4.4 | −24.3 | 190 | Simkus et al. (2016) | 3 |
| S. Africa | Evander | EV522 FW 030801HWD | 1694.0 | −5.63 | −27.7 | 2330 | Lippmann et al. (2003) | 3 |
| S. Africa | Evander | EV818 FW 030601 | 1950.0 | −10.24 | −35.9 | 9106 | Lippmann et al. (2003) | 3 |
| S. Africa | Evander | EV811 FW 030501 | 1340.0 | −5.02 | −30.0 | 612 | Lippmann et al. (2003) | 3 |
| S. Africa | Evander | EV818 FW 062101 | 1950.0 | −10.87 | −36.9 | 8544 | Lippmann et al. (2003) | 3 |
| S. Africa | Evander | EV219 H1 030901 ED | 1474.0 | −4.98 | −30.1 | 1364 | Onstott et al. (2006) | 3 |
| S. Africa | Evander | EV219 H5 030901 ED | 1474.0 | −4.92 | −27.6 | 810 | Onstott et al. (2006) | 3 |
| S. Africa | Evander | EV221 H1 052102 | 1624.0 | −5.86 | −29.7 | 1048 | Onstott et al. (2006) | 3 |
| S. Africa | Evander | EV221 H2 111601 | 1624.0 | −4.37 | −17.9 | 2732 | Onstott et al. (2006) | 3 |
| S. Africa | Evander | EV221 H3 111601 | 1624.0 | −5.97 | −30.0 | 1682 | Onstott et al. (2006) | 3 |
| S. Africa | Evander | EV522 H1 041801CTS | 1694.0 | −6.48 | −30.9 | 3776 | Onstott et al. (2006) | 3 |
| S. Africa | Evander | EV522 H2 041801CTS | 1694.0 | −6.19 | −30.4 | nm | | 3 |

(*continued on next page*)

**Table A1** (*continued*)

| Country | Location | Sample ID | Depth (m) | $\partial^{18}O$ | $\partial^{2}H$ | TDS (mg/L) | Source | Sampling Method |
|---|---|---|---|---|---|---|---|---|
| | | | | | | | Onstott et al. (2006) | |
| S. Africa | Evander | EV813 FW 030601 | 1410.0 | −4.75 | −30.3 | nm | Onstott et al. (2006) | 3 |
| S. Africa | Evander | EV818 FW 030601 | 1950.0 | −10.24 | −35.9 | 9106 | Onstott et al. (2006) | 3 |
| S. Africa | Evander | EV818 FW 051001 | 1950.0 | −10.50 | −36.2 | 8770 | Onstott et al. (2006) | 3 |
| S. Africa | Evander | EV820 FW 061802 | 2005.0 | −6.74 | −30.0 | 2115 | Onstott et al. (2006) | 3 |
| S. Africa | Evander | EV820 FW 121401 | 2005.0 | −6.75 | −31.2 | 2530 | Onstott et al. (2006) | 3 |
| S. Africa | Evander | EV821 FW 101601 | 2055.0 | −7.44 | −29.1 | 5292 | Onstott et al. (2006) | 3 |
| S. Africa | Evander | EV914 FW 022801 ED | 1400.0 | −4.68 | −31.2 | 632 | Onstott et al. (2006) | 3 |
| S. Africa | Kloof | KL739 FW 062901 | 3100.0 | −7.24 | −20.4 | 13,218 | Lippmann et al. (2003) | 3 |
| S. Africa | Kloof | KL441 HWDS H1 120198 | 3082.0 | −5.71 | −27.7 | 3221 | Lippmann et al. (2003) | 3 |
| S. Africa | Kloof | KL441 HWDN FW 022801 | 3300.0 | −9.88 | −28.8 | 9004 | Onstott et al. (2006) | 3 |
| S. Africa | Kloof | KL441 HWDS H1 050201 | 3300.0 | −4.39 | −30.9 | 2236 | Onstott et al. (2006) | 3 |
| S. Africa | Kloof | KL441 HWDS H2 050201 | 3300.0 | −4.80 | −27.9 | 2523 | Onstott et al. (2006) | 3 |
| S. Africa | Kloof | KL441 HWDS H2 100201 | 3300.0 | −5.04 | −27.9 | 2315 | Onstott et al. (2006) | 3 |
| S. Africa | Kloof | KL441 HWDS H3 111401 | 3300.0 | −5.03 | −27.5 | 2037 | Onstott et al. (2006) | 3 |
| S. Africa | Kloof | KL443 HWDN FW 030501 | 3400.0 | −10.48 | −29.2 | nm | Onstott et al. (2006) | 3 |
| S. Africa | Kloof | KL443 HWDN FW 050801 | 3400.0 | −11.10 | −33.8 | 16,447 | Onstott et al. (2006) | 3 |
| S. Africa | Kloof | KL445 | 3280.0 | −9.4 | −31.8 | 11,100 | Simkus et al. (2016) | 3 |
| S. Africa | Masimong | MM51870 FW 030402 | 1880.0 | −6.52 | −38.0 | 2670 | Onstott et al. (2006) | 3 |
| S. Africa | Masimong | MM51940 FW 200712 | 1900.0 | −7.0 | −40.0 | nm | Lau et al. (2014) | 3 |
| S. Africa | Masimong | MM51940 | 1900.0 | −7.0 | −40.1 | nm | Heard et al. (2018) | 3 |
| S. Africa | Middelbult | MB FW 040301 Sec33 | 200.0 | −3.43 | −27.6 | nm | Onstott et al. (2006) | 3 |
| S. Africa | Middelbult | MB FW 040301 Sec49 | 200.0 | −3.06 | −25.5 | 776 | Onstott et al. (2006) | 3 |
| S. Africa | Moab | MK1200–21/06/18 18O—2H H2O | nm | −4.0 | −23.9 | nm | Unpub. | 3 |
| S. Africa | Moab | MK101–16/06/18 18O—2H H2O | nm | −12.3 | −22.8 | nm | Unpub. | 3 |
| S. Africa | Moab | MK070818 101 LVL WATER ISOTOPES | nm | −11.9 | −8.4 | nm | Unpub. | 3 |
| S. Africa | Moab | MK190618 101 LVL WATER ISOTOPES | nm | −11.8 | −9.4 | nm | Unpub. | 3 |
| S. Africa | Moab | MK210618 1200 level WATER ISOTOPES | nm | −4.0 | −24.1 | nm | Unpub. | 3 |
| S. Africa | Moab | MK231018 95 LVL WATER ISOTOPES | nm | −11.7 | −26.4 | nm | Unpub. | 3 |
| S. Africa | Moab | 11.07.19_MKL95_LibA_D0 | nm | −12.2 | −25.4 | nm | Unpub. | 3 |
| S. Africa | Moab | 17.07.19_MKL95_LibA_D0 | nm | −12.3 | −25.8 | nm | Unpub. | 3 |
| S. Africa | Moab | 10.07.19_MKL101_Barminco | nm | −12.4 | −16.8 | nm | Unpub. | 3 |
| S. Africa | Mponeng | MP104 E65XC H1 | 2825.0 | −6.82 | −29.1 | 3146 | Onstott et al. (2006) | 3 |
| S. Africa | Mponeng | MP104 E65XC H1 | 2825.0 | −6.92 | −29.1 | 4236 | Onstott et al. (2006) | 3 |
| S. Africa | Mponeng | MP109 BH1 070196 | 3198.0 | −5.25 | −27.4 | 676 | Onstott et al. (2006) | 3 |
| S. Africa | Mponeng | MP109 FW 101701 | 3305.0 | −6.96 | −30.4 | 11,738 | Onstott et al. (2006) | 3 |
| S. Africa | Mponeng | MS151 FW 022202 | 2028.0 | −7.19 | −43.4 | 3865 | Onstott et al. (2006) | 3 |
| S. Africa | Tau Tona | TT100 FW 082702 | 3025.0 | −4.89 | −25.7 | 185 | Onstott et al. (2006) | 3 |
| S. Africa | Tau Tona | TT107FR240811 | 3048.0 | −5.1 | −22.4 | nm | Lau et al. (2014) | 3 |
| S. Africa | Tau Tona | TT109FW060312BH2 | 3136.0 | −5.0 | −25.3 | nm | Lau et al. (2014) | 3 |
| S. Africa | Tau Tona | TT109 Bh2 | 3140.0 | −5.0 | −25.3 | 300 | Simkus et al. (2016) | 3 |
| S. Africa | Tau Tona | TT107 | 3050.0 | −4.8 | −24.4 | 200 | Simkus et al. (2016) | 3 |
| Finland | Enonkoski | 17092 | 0.0 | −13.7 | −91.4 | 17,385 | Unpub. | 3 |
| Finland | Enonkoski | 17093 | 14.0 | −13.6 | −90.9 | 18,026 | Unpub. | 3 |
| Finland | Enonkoski | 17094 | 0.0 | −13.5 | −90.4 | 18,916 | Unpub. | 3 |
| Finland | Enonkoski | 17095 | 14.0 | −13.2 | −81.2 | 27,635 | Frape et al. (2003) | 3 |

(*continued on next page*)

**Table A1** (*continued*)

| Country | Location | Sample ID | Depth (m) | $\partial^{18}O$ | $\partial^{2}H$ | TDS (mg/L) | Source | Sampling Method |
|---|---|---|---|---|---|---|---|---|
| Finland | Enonkoski | 17106 | 0.0 | −13.9 | −98.4 | 13,749 | Unpub. | 3 |
| Finland | Enonkoski | 17107 | 101.2 | −14.5 | −98.2 | 11,708 | Frape et al. (2003) | 3 |
| Finland | Enonkoski | 17108 | 200.0 | −13.2 | −83.5 | 20,119 | Unpub. | 3 |
| Finland | Enonkoski | 17109 | 301.5 | −13.3 | −83.6 | 25,049 | Unpub. | 3 |
| Finland | Enonkoski | 17110 | 405.8 | −13.4 | −82.4 | 23,734 | Unpub. | 3 |
| Sweden | Klipperas | GTL K1 9 | 11.0 | −11.7 | −93.8 | 400 | Unpub. | 2 |
| Sweden | Klipperas | GTL K1 9 | 61.0 | −13.5 | −105.8 | 5890 | Unpub. | 2 |
| Finland | Kerimaki | | 140.0 | −13.4 | −94.4 | 60 | Nurmi et al. (1988) | 2 |
| Finland | Kerimaki | | 540.0 | −13.5 | −93.9 | 3900 | Nurmi et al. (1988) | 2 |
| Finland | Kerimaki | | 700.0 | −13.7 | −95.4 | 5300 | Nurmi et al. (1988) | 2 |
| Finland | Liminka | | 100.0 | −14.5 | −106.0 | 6200 | Nurmi et al. (1988) | 2 |
| Finland | Liminka | | 400.0 | −12.7 | −88.8 | 16,100 | Nurmi et al. (1988) | 2 |
| Finland | Liminka | | 600.0 | −12.2 | −84.2 | 37,200 | Nurmi et al. (1988) | 2 |
| Finland | Liminka | | 720.0 | −12.1 | −81.0 | 41,000 | Nurmi et al. (1988) | 2 |
| Finland | Miihkali | | 250.0 | −10.4 | −30.3 | 40,077 | Unpub. | 2 |
| Finland | Miihkali | | 502.0 | −10.4 | −28.2 | 40,680 | Frape et al. (2003) | 2 |
| Finland | Miihkali | | 745.0 | −10.2 | −20.8 | 38,516 | Unpub. | 2 |
| Finland | Miihkali | | 889.0 | −11.8 | −15.8 | 146,561 | Unpub. | 2 |
| Finland | Miihkali | | 90.0 | −10.5 | −18.7 | 38,764 | Unpub. | 2 |
| Finland | Miihkali | | 340.0 | −10.5 | −19.2 | 41,860 | Unpub. | 2 |
| Finland | Miihkali | | 590.0 | −10.2 | −21.2 | 40,350 | Unpub. | 2 |
| Finland | Miihkali | | 790.0 | −10.8 | −21.1 | 64,559 | Unpub. | 2 |
| Finland | Miihkali | | 940.0 | −11.7 | −25.7 | 147,271 | Unpub. | 2 |
| Finland | Miihkali | | 990.0 | −11.8 | −18.0 | 148,435 | Unpub. | 2 |
| Finland | Miihkali | | 1040.0 | −12.4 | −22.7 | nm | Unpub. | 2 |
| Finland | Miihkali | | 1100.0 | −11.7 | −11.8 | 149,380 | Unpub. | 2 |
| Finland | Miihkali | | 130–180 | −10.1 | −9.4 | nm | Unpub. | 2 |
| Finland | Miihkali | | 180–230 | −10.3 | −10.7 | nm | Unpub. | 2 |
| Finland | Miihkali | | 330–380 | −10.4 | −11.5 | nm | Unpub. | 2 |
| Finland | Miihkali | | 380–430 | −10.4 | −11.2 | nm | Unpub. | 2 |
| Finland | Miihkali | | 530–580 | −10.3 | −10.2 | nm | Unpub. | 2 |
| Finland | Miihkali | | 580–630 | −10.4 | −11.2 | nm | Unpub. | 2 |
| Finland | Miihkali | | 780–830 | −10.6 | −10.2 | nm | Unpub. | 2 |
| Finland | Miihkali | | 830–880 | −11.8 | −10.9 | nm | Unpub. | 2 |
| Finland | Miihkali | | 930–980 | −11.7 | −9.1 | nm | Unpub. | 2 |
| Finland | Miihkali | | 980–1030 | −11.7 | −10.7 | nm | Unpub. | 2 |
| Finland | Miihkali | 17071 | 15.0 | −10.3 | −15.8 | 37,676 | Unpub. | 2 |
| Finland | Miihkali | 17072 | 102.1 | −10.4 | −14.8 | 35,139 | Unpub. | 2 |
| Finland | Miihkali | 17073 | 252.7 | −10.5 | −12.7 | 34,662 | Unpub. | 2 |
| Finland | Miihkali | 17074 | 500.9 | −10.5 | −13.1 | 33,791 | Unpub. | 2 |
| Finland | Miihkali | 17075 | 750.0 | −10.4 | −12.5 | 34,275 | Frape et al. (2003) | 2 |
| Finland | Miihkali | 17076 | 966.7 | −12.0 | −7.6 | 136,132 | Unpub. | 2 |
| Finland | Miihkali | 17077 | 15.0 | −12.9 | −78.3 | 9536 | Unpub. | 2 |
| Finland | Miihkali | 17083 | 10.0 | −13.5 | −101.3 | 110 | Unpub. | 2 |
| Finland | Miihkali | 17084 | 200.6 | −13.4 | −99.2 | 132 | Unpub. | 2 |
| Finland | Miihkali | 17085 | 300.6 | −13.0 | −87.6 | 10,288 | Unpub. | 2 |
| Finland | Miihkali | 17086 | 401.2 | −13.1 | −87.5 | 10,956 | Unpub. | 2 |
| Finland | Miihkali | 17079 | 15.0 | −13.5 | −94.2 | 9266 | Unpub. | 2 |
| Finland | Miihkali | 17078 | 15.0 | −13.8 | −101.7 | nm | Unpub. | 2 |
| Finland | Miihkali | 17080 | 15.0 | −13.3 | −99.1 | 174 | Unpub. | 2 |
| Finland | Miihkali | 17081 | 0.0 | −11.7 | −95.2 | nm | Unpub. | 2 |
| Finland | Noormarkku | 17063 | 13.0 | −11.3 | −85.9 | 1643 | Unpub. | 2 |
| Finland | Noormarkku | 17064 | 101.5 | −11.6 | −89.0 | 7613 | Unpub. | 2 |
| Finland | Noormarkku | 17065 | 201.2 | −11.6 | −89.0 | 10,521 | Unpub. | 2 |
| Finland | Noormarkku | 17066 | 300.9 | −12.3 | −92.2 | 15,572 | Unpub. | 2 |
| Finland | Noormarkku | 17067 | 404.6 | −12.3 | −92.2 | 17,903 | Unpub. | 2 |
| Finland | Noormarkku | 17068 | 500.0 | −11.2 | −78.9 | 37,418 | Unpub. | 2 |
| Finland | Noormarkku | 17069 | 533.3 | −11.1 | −76.7 | 40,769 | Unpub. | 2 |
| Finland | Noormarkku | 17070 | 559.4 | −11.3 | −77.8 | 37,835 | Unpub. | 2 |
| Finland | Vammala | 17089 | 0.0 | −13.8 | −104.0 | 2857 | Unpub. | 3 |
| Finland | Vammala | 17090 | 0.0 | −14.6 | −109.3 | 1782 | Unpub. | 3 |
| Finland | Vammala | 17091 | 0.0 | −15.1 | −110.8 | 1815 | Unpub. | 3 |
| Finland | Outukumpu | 17087 | 15.0 | −13.9 | −105.4 | 80 | Unpub. | 2 |
| Finland | Outukumpu | 17088 | 450.6 | −13.8 | −106.3 | 390 | Unpub. | 2 |
| Finland | Outukumpu | | 270.0 | −13.9 | −98.8 | 100 | Nurmi et al. (1988) | 2 |
| Finland | Outukumpu | | 600.0 | −14.4 | −102.1 | 13,400 | Nurmi et al. (1988) | 2 |
| Finland | Outukumpu | | 770.0 | −14.3 | −101.5 | 13,700 | Nurmi et al. (1988) | 2 |
| Finland | Outukumpu | | 1010.0 | −13.0 | −74.8 | 26,500 | Nurmi et al. (1988) | 2 |
| Finland | Outukumpu | | 1070.0 | −13.0 | −73.4 | 27,100 | Nurmi et al. (1988) | 2 |
| Finland | Outukumpu | S8706701 | 290.0 | −14.4 | −105.5 | 198 | Unpub. | 2 |
| Finland | Outukumpu | S8706702 | 606.0 | −14.3 | −105.1 | 7570 | Unpub. | 2 |
| Finland | Outukumpu | S8706703 | 787.0 | −14.2 | −105.3 | 7762 | Unpub. | 2 |
| Finland | Outukumpu | S8706713 | 854.0 | −13.5 | −95.4 | 17,095 | Unpub. | 2 |
| Finland | Outukumpu | S8706704 | 244.0 | −13.9 | −104.6 | 116 | Unpub. | 2 |
| Finland | Outukumpu | S8706705 | 402.0 | −14.1 | −102.1 | 223 | Unpub. | 2 |

(*continued on next page*)

**Table A1** (*continued*)

| Country | Location | Sample ID | Depth (m) | $\partial^{18}O$ | $\partial^{2}H$ | TDS (mg/L) | Source | Sampling Method |
|---|---|---|---|---|---|---|---|---|
| Finland | Outukumpu | S8706706a | 697.0 | −14.4 | −102.3 | 12,870 | Frape et al. (2003) | 2 |
| Finland | Outukumpu | S8706706b | 700.0 | −14.4 | −102.9 | nm | Unpub. | 2 |
| Finland | Outukumpu | S8706707 | 1036.0 | −12.9 | −80.1 | 27,908 | Unpub. | 2 |
| Finland | Outukumpu | S8706708 | 1178.0 | −12.9 | −80.1 | 28,122 | Frape et al. (2003) | 2 |
| Finland | Outukumpu Deep Drill Hole | OK-1 | 25.0 | −12.1 | −79.0 | 12,900 | Kietäväinen et al. (2013) | 2 |
| Finland | Outukumpu Deep Drill Hole | OK-2 | 100.0 | −12.5 | −82.0 | 10,900 | Kietäväinen et al. (2013) | 2 |
| Finland | Outukumpu Deep Drill Hole | OK-3 | 200.0 | −12.6 | −83.0 | 11,800 | Kietäväinen et al. (2013) | 2 |
| Finland | Outukumpu Deep Drill Hole | OK-4 | 300.0 | −12.7 | −83.0 | 11,200 | Kietäväinen et al. (2013) | 2 |
| Finland | Outukumpu Deep Drill Hole | OK-5 | 400.0 | −12.9 | −83.0 | 12,600 | Kietäväinen et al. (2013) | 2 |
| Finland | Outukumpu Deep Drill Hole | OK-6 | 500.0 | −12.9 | −83.0 | 12,100 | Kietäväinen et al. (2013) | 2 |
| Finland | Outukumpu Deep Drill Hole | OK-7 | 600.0 | −12.9 | −83.0 | 12,200 | Kietäväinen et al. (2013) | 2 |
| Finland | Outukumpu Deep Drill Hole | OK-8 | 700.0 | −13.0 | −83.0 | 12,700 | Kietäväinen et al. (2013) | 2 |
| Finland | Outukumpu Deep Drill Hole | OK-9 | 800.0 | −13.0 | −83.0 | 13,100 | Kietäväinen et al. (2013) | 2 |
| Finland | Outukumpu Deep Drill Hole | OK-10 | 900.0 | −12.9 | −83.0 | 13,100 | Kietäväinen et al. (2013) | 2 |
| Finland | Outukumpu Deep Drill Hole | OK-11 | 1000.0 | −12.9 | −83.0 | 12,700 | Kietäväinen et al. (2013) | 2 |
| Finland | Outukumpu Deep Drill Hole | OK-12 | 1100.0 | −12.9 | −83.0 | 13,700 | Kietäväinen et al. (2013) | 2 |
| Finland | Outukumpu Deep Drill Hole | OK-13 | 1200.0 | −12.8 | −83.0 | 13,000 | Kietäväinen et al. (2013) | 2 |
| Finland | Outukumpu Deep Drill Hole | OK-14 | 1300.0 | −12.7 | −82.0 | 12,400 | Kietäväinen et al. (2013) | 2 |
| Finland | Outukumpu Deep Drill Hole | OK-15 | 1400.0 | −12.2 | −80.0 | 12,600 | Kietäväinen et al. (2013) | 2 |
| Finland | Outukumpu Deep Drill Hole | OK-16 | 1500.0 | −11.2 | −73.0 | 14,700 | Kietäväinen et al. (2013) | 2 |
| Finland | Outukumpu Deep Drill Hole | OK-17 | 1600.0 | −10.9 | −69.0 | 21,800 | Kietäväinen et al. (2013) | 2 |
| Finland | Outukumpu Deep Drill Hole | OK-18 | 1700.0 | −10.5 | −61.0 | 35,400 | Kietäväinen et al. (2013) | 2 |
| Finland | Outukumpu Deep Drill Hole | OK-19 | 1800.0 | −10.4 | −58.0 | 43,900 | Kietäväinen et al. (2013) | 2 |
| Finland | Outukumpu Deep Drill Hole | OK-20 | 1900.0 | −10.5 | −57.0 | 48,700 | Kietäväinen et al. (2013) | 2 |
| Finland | Outukumpu Deep Drill Hole | OK-21 | 2000.0 | −10.5 | −60.0 | 50,600 | Kietäväinen et al. (2013) | 2 |
| Finland | Outukumpu Deep Drill Hole | OK-22 | 2100.0 | −10.6 | −62.0 | 46,200 | Kietäväinen et al. (2013) | 2 |
| Finland | Outukumpu Deep Drill Hole | OK-23 | 2200.0 | −10.6 | −64.0 | 41,500 | Kietäväinen et al. (2013) | 2 |
| Finland | Outukumpu Deep Drill Hole | OK-24 | 2300.0 | −10.8 | −65.0 | 42,300 | Kietäväinen et al. (2013) | 2 |
| Finland | Outukumpu Deep Drill Hole | OK-25 | 2400.0 | −11.0 | −70.0 | 64,400 | Kietäväinen et al. (2013) | 2 |
| Finland | Outukumpu Deep Drill Hole | OKU2260-G1 | 2260.0 | −10.9 | −70.7 | nm | Kietäväinen et al. (2017) | 1 |
| Finland | Outukumpu Deep Drill Hole | OKU2260-G3 | 2260.0 | −10.9 | −70.7 | nm | Kietäväinen et al. (2017) | 1 |
| Finland | Outukumpu Deep Drill Hole | OKU2260-G7 | 2260.0 | −11.0 | −69.2 | nm | Kietäväinen et al. (2017) | 1 |
| Finland | Outukumpu Deep Drill Hole | OKU2260-G10 | 2260.0 | −11.0 | −69.2 | nm | Kietäväinen et al. (2017) | 1 |
| Finland | Outukumpu Deep Drill Hole | OKU500-G3 | 500.0 | −13.1 | −82.8 | 11,000 | Kietäväinen et al. (2017) | 1 |
| Finland | Outukumpu Deep Drill Hole | OKU500-G4 | 500.0 | −13.1 | −82.8 | Nm | Kietäväinen et al. (2017) | 1 |
| Finland | Outukumpu Deep Drill Hole | OKU500-G8 | 500.0 | −13.1 | −82.9 | 11,000 | Kietäväinen et al. (2017) | 1 |
| Finland | Outukumpu Deep Drill Hole | OKU500-G12 | 500.0 | −13.1 | −82.7 | Nm | Kietäväinen et al. (2017) | 1 |
| Finland | Outukumpu Deep Drill Hole | OKU2300-G1 | 2300.0 | −10.56 | −65.4 | Nm | Kietäväinen et al. (2017) | 1 |
| Finland | Outukumpu Deep Drill Hole | OKU1820-G1 | 1820.0 | −10.47 | −56.0 | 38,000 | Kietäväinen et al. (2017) | 1 |
| Finland | | OUTO-500 (6) | 500.0 | −13.11 | −82.9 | 12,000 | | 2 |

(*continued on next page*)

**Table A1** (*continued*)

| Country | Location | Sample ID | Depth (m) | $\partial^{18}O$ | $\partial^{2}H$ | TDS (mg/L) | Source | Sampling Method |
|---|---|---|---|---|---|---|---|---|
| | Outukumpu Deep Drill Hole | | | | | | Kietäväinen et al. (2017) | |
| Finland | Outukumpu Deep Drill Hole | OUTO-970 (2) | 970.0 | −12.94 | −82.8 | 12,000 | Kietäväinen et al. (2017) | 2 |
| Finland | Outukumpu Deep Drill Hole | OUTO-1470 (8) | 1470.0 | −10.84 | −70.8 | 14,000 | Kietäväinen et al. (2017) | 2 |
| Finland | Outukumpu Deep Drill Hole | OUTO-1820 (4) | 1820.0 | −10.59 | −56.6 | 51,000 | Kietäväinen et al. (2017) | 2 |
| Finland | Outukumpu Deep Drill Hole | OUTO-2350 (7) | 2350.0 | −11.06 | −69.9 | 57,000 | Kietäväinen et al. (2017) | 2 |
| Finland | Outukumpu Deep Drill Hole | OUTO-2480 (5) | 2480.0 | −11.30 | −66.0 | 69,000 | Kietäväinen et al. (2017) | 2 |
| Finland | Outukumpu Deep Drill Hole | OU-1 | 25.0 | −12.00 | −84.8 | 7000 | Kietäväinen et al. (2017) | 2 |
| Finland | Outukumpu Deep Drill Hole | OU-3A | 200.0 | −12.38 | −86.5 | 7000 | Kietäväinen et al. (2017) | 2 |
| Finland | Outukumpu Deep Drill Hole | OU-4A | 300.0 | −12.69 | −85.4 | 7000 | Kietäväinen et al. (2017) | 2 |
| Finland | Outukumpu Deep Drill Hole | OU-5A | 400.0 | −12.95 | −83.5 | 11,000 | Kietäväinen et al. (2017) | 2 |
| Finland | Outukumpu Deep Drill Hole | OU-6A | 500.0 | −13.05 | −82.8 | 11,000 | Kietäväinen et al. (2017) | 2 |
| Finland | Outukumpu Deep Drill Hole | OU-7A | 600.0 | −12.98 | −82.6 | 12,000 | Kietäväinen et al. (2017) | 2 |
| Finland | Outukumpu Deep Drill Hole | OU-8A | 700.0 | −13.11 | −83.0 | 12,000 | Kietäväinen et al. (2017) | 2 |
| Finland | Outukumpu Deep Drill Hole | OU-9A | 800.0 | −13.06 | −83.1 | 12,000 | Kietäväinen et al. (2017) | 2 |
| Finland | Outukumpu Deep Drill Hole | OU-10A | 900.0 | −13.01 | −82.8 | 12,000 | Kietäväinen et al. (2017) | 2 |
| Finland | Outukumpu Deep Drill Hole | OU-11A | 1000.0 | −13.11 | −82.6 | 12,000 | Kietäväinen et al. (2017) | 2 |
| Finland | Outukumpu Deep Drill Hole | OKU180-G1 | 180.0 | −12.54 | −87.2 | 8000 | Kietäväinen et al. (2017) | 1 |
| Finland | Outukumpu Deep Drill Hole | OKU180-G2 | 180.0 | −12.68 | −87.0 | 7000 | Kietäväinen et al. (2017) | 1 |
| Finland | Outukumpu Deep Drill Hole | OKU180-G3 | 180.0 | −12.79 | −85.7 | 8000 | Kietäväinen et al. (2017) | 1 |
| Finland | Outukumpu Deep Drill Hole | OKU180-G6 | 180.0 | −12.57 | −88.6 | 6000 | Kietäväinen et al. (2017) | 1 |
| Finland | Outukumpu Deep Drill Hole | OKU180-G7 | 180.0 | −12.61 | −88.4 | 5000 | Kietäväinen et al. (2017) | 1 |
| Finland | Outukumpu Deep Drill Hole | OKU180/25 | 180.0 | −12.55 | −88.8 | nm | Kietäväinen et al. (2017) | 2 |
| Finland | Outukumpu Deep Drill Hole | OKU180/27 | 180.0 | −12.55 | −88.8 | nm | Kietäväinen et al. (2017) | 2 |
| Sweden | Parainen | | 280.0 | −11.5 | −26.3 | 250 | Nurmi et al. (1988) | 2 |
| Sweden | Parainen | | 410.0 | −11.3 | −76.1 | 1000 | Nurmi et al. (1988) | 2 |
| Sweden | Parainen | | 490.0 | −9.8 | −67.7 | 6500 | Nurmi et al. (1988) | 2 |
| Finland | Pori | 17096 | 0.0 | −15.6 | −115.8 | 2773 | Unpub. | 2 |
| Finland | Pori | 17097 | 15.2 | −15.5 | −118.1 | 2716 | Unpub. | 2 |
| Finland | Pori | 17098 | 48.5 | −15.6 | −118.3 | 2662 | Unpub. | 2 |
| Finland | Pori | 17099 | 100.0 | −15.5 | −116.6 | 7318 | Unpub. | 2 |
| Finland | Pori | 17100 | 145.5 | −14.0 | −105.6 | 4490 | Unpub. | 2 |
| Finland | Pori | 17101 | 200.0 | −13.4 | −102.8 | 4879 | Frape et al. 2003 | 2 |
| Finland | Pori | 17102 | 250.0 | −10.6 | −65.1 | 49,411 | Unpub. | 2 |
| Finland | Pori | 17103 | 266.7 | −9.0 | −55.6 | 69,936 | Unpub. | 2 |
| Finland | Pori | 17104 | 400.0 | −10.7 | −73.3 | 36,583 | Unpub. | 2 |
| Finland | Pori | 17105 | 401.5 | −8.4 | −47.9 | 79,325 | Unpub. | 2 |
| Finland | Pori-P0–1 | S8706722 | 0.0 | −15.6 | −117.1 | 2640 | Unpub. | 2 |
| Finland | Pori-P0–1 | S8706723 | 52.0 | −16.8 | −121.0 | 2780 | Unpub. | 2 |
| Finland | Pori-P0–1 | S8706724 | 111.0 | −20.7 | −125.7 | 2689 | Frape et al. 2003 | 2 |
| Finland | Pori-P0-1 | S8706725 | 151.0 | −13.6 | −109.0 | 4554 | Unpub. | 2 |
| Finland | Pori-P0–1 | S8706726 | 201.0 | −12.8 | −101.7 | 5801 | Unpub. | 2 |
| Finland | Pori-P0–1 | S8706727 | 241.0 | −9.4 | −52.1 | 69,072 | Unpub. | 2 |
| Finland | Pori-P0–1 | S8706728 | 301.0 | −8.3 | −46.3 | 91,393 | Unpub. | 2 |
| Finland | Pori-P0–1 | S8706729 | 351.0 | −7.9 | −56.1 | 93,752 | Unpub. | 2 |
| Finland | Pori-P0–1 | S8706730 | 402.0 | −8.1 | −54.4 | 92,030 | Unpub. | 2 |
| Finland | Pori-P0–1 | 12930 | 410.0 | −7.9 | −44.6 | 148,554 | Unpub. | 2 |
| Finland | Pori-P0–1 | | 440.0 | −8.1 | −44.6 | nm | Unpub. | 2 |
| Finland | Pori-P0–1 | 12932 | 480.0 | −7.7 | −45.4 | 119,645 | Unpub. | 2 |
| Finland | Pori-P0–1 | 12933 | 530.0 | −8.1 | −48.7 | 24,706 | Unpub. | 2 |
| Finland | Pori-P0–1 | 12934 | 580.0 | −7.7 | −43.9 | 127,254 | Unpub. | 2 |
| Finland | Pyhäsalmi | | 2400.0 | −12.27 | −70.2 | 66,900 | Miettinen et al. 2015 | 3 |

(*continued on next page*)

**Table A1** (*continued*)

| Country | Location | Sample ID | Depth (m) | $\partial^{18}O$ | $\partial^{2}H$ | TDS (mg/L) | Source | Sampling Method |
|---|---|---|---|---|---|---|---|---|
| Finland | Pyhäsalmi | | 2400.0 | −12.27 | −70.2 | 66,900 | Miettinen et al. 2015 | 3 |
| Finland | Pyhäsalmi | | 1910.0 | −13.70 | −91.2 | 25,700 | Miettinen et al. 2015 | 3 |
| Finland | Ylivieska | S8706714 | 202.0 | −13.0 | −97.7 | 422 | Unpub. | 2 |
| Finland | Ylivieska | S8706715 | 302.0 | −12.8 | −93.5 | 4174 | Unpub. | 2 |
| Finland | Ylivieska | S8706716 | 543.0 | −13.2 | −57.0 | 45,670 | Unpub. | 2 |
| Finland | Ylivieska | S8706717 | 618.0 | −13.4 | −42.8 | 75,759 | Unpub. | 2 |
| Finland | Ylivieska | | 640.0 | −13.1 | −54.8 | 54,927 | Unpub. | 2 |
| Finland | Ylivieska | S8706718 | 101.0 | −12.5 | −94.0 | 857 | Unpub. | 2 |
| Finland | Ylivieska | S8706719 | 200.0 | −13.1 | −100.5 | 2838 | Unpub. | 2 |
| Finland | Ylivieska | S8706720 | 300.0 | −12.8 | −99.0 | 5184 | Unpub. | 2 |
| Finland | Ylivieska | S8706721 | 400.0 | −13.5 | −97.4 | 19,753 | Unpub. | 2 |
| Finland | Ylivieska | 17059 | 240.3 | −13.2 | −99.4 | nm | Unpub. | 2 |
| Finland | Ylivieska | 17060 | 357.3 | −13.1 | −45.6 | 53,660 | Frape et al. 2003 | 2 |
| Finland | Ylivieska | 17061 | 437.9 | −12.8 | −84.9 | nm | Unpub. | 2 |
| Finland | Ylivieska | 17062 | 590.3 | −13.7 | −26.7 | nm | Unpub. | 2 |

**Table A2**
Water isotope data from service water (waters introduced into the mine for use in drilling and mine operations).

| Country | Location | Sample ID | $\partial^{18}O$ | $\partial^{2}H$ | Source |
|---|---|---|---|---|---|
| Canada | Kidd Creek Mine, Timmins | 10.05.06_KC_8800_Refuge_Drilling Water | −12.1 | −91.6 | Unpub. |
| Canada | Kidd Creek Mine, Timmins | 1.04.2009_KC_7850_Service water | −11.2 | −96 | Unpub. |
| Canada | Kidd Creek Mine, Timmins | 12.01.2010_KC_7850_Service water | −11 | −89.8 | Unpub. |
| Canada | Kidd Creek Mine, Timmins | 01.03.2012_KC_9500_service water | −11.8 | −90.1 | Unpub. |
| Canada | Kidd Creek Mine, Timmins | 14.06.2012KCL9500_BHY13762-Service Water | −12.5 | −87.6 | Unpub. |
| Canada | Kidd Creek Mine, Timmins | 22.10.2015_KCL7850_ServiceWater | −11.4 | −90.4 | Unpub. |
| Canada | Kidd Creek Mine, Timmins | 12.07.2016_KCL7850_SW (service water) | −12.6 | −91.1 | Unpub. |
| Canada | Kidd Creek Mine, Timmins | 24.01.2017_KCL7850_SW | −10.6 | −80.8 | Unpub. |
| Canada | Kidd Creek Mine, Timmins | 06.06.2017_KCL7850_SW | −12.4 | −89.8 | Unpub. |
| Canada | Kidd Creek Mine, Timmins | 29.01.2018_KCL7850_SW | −10.7 | −83.1 | Unpub. |
| Canada | Kidd Creek Mine, Timmins | 14.6.2018-KC7850-SW | −13 | −94.3 | Unpub. |
| Canada | Kidd Creek Mine, Timmins | 05.02.2019_KC7850_SW | −11.3 | −83.3 | Unpub. |
| Canada | Nickel Rim South Mine, Sudbury | 29.11.2013_NR_1730m_Service Water | −10.3 | −72.9 | Unpub. |
| Canada | Nickel Rim South Mine, Sudbury | 22.10.2014_NR_1730m_Service water | −10.1 | −74.1 | Unpub. |
| Canada | Nickel Rim South Mine, Sudbury | 29.11.2014_NR_1730m_Service water | −10.3 | −72.9 | Unpub. |
| Canada | Birchtree Mine, Thompson | 28.05.2007_BT3950L_Service water | −13.4 | −112.1 | Unpub. |
| Canada | Thompson Mine, Thompson | | −12.8 | −108.4 | Unpub. |
| Canada | Thompson Mine, Thompson | | −12.9 | −112.2 | Unpub. |
| South Africa | Beatrix | BE223 SW 031301 | −6.22 | −42.2 | Onstott et al. (2006) |
| South Africa | Driefontein | DR548 SW1 090198 | −2.68 | −8.6 | Onstott et al. (2006) |
| South Africa | Driefontein | DR548 SW2 120198 | −2.17 | −8.1 | Onstott et al. (2006) |
| South Africa | Evander | EV219 SW 030901 | −4.59 | −25.8 | Onstott et al. (2006) |
| South Africa | Evander | EV224 SW1&2081302 | −4.65 | −20.7 | Onstott et al. (2006) |
| South Africa | Evander | EV818 SW 030601 | −3.87 | −19.3 | Onstott et al. (2006) |

## References


Artemieva, I.M., Mooney, W.D., 2001. Thermal thickness and evolution of Precambrian lithosphere: a global study. J. Geophys. Res. 106, 16387–16414.

Ballentine, C.J., Burnard, P.G., 2002. Production, release and transport of noble gases in the continental crust. In: Porcelli, D., Ballentine, C.J., Wieler, R. (Eds.), Noble Gases in Geochemistry and Cosmochemistry, Reviews in Mineralogy and Geochemistry. Mineralogical Society of America, pp. 481–538.

Barrett, T.J., Wilson, G.C., Hamilton, M.A., Kontak, D.J., Burns, M., Ayer, J.A., Stott, G., 2013. 13. The Montcleg gold deposit, Abitibi greenstone belt, east Timmins region, Ontario: Stratigraphy, lithogeochemistry, mineralization and nature of vein fluids. In: Ontario Geological Survey Publication MRD300.

Beaty, D.W., Taylor, H.P., Coad, P.R., 1988. An oxygen isotope study of the Kidd Creek, Ontario volcanogenic massive sulfide deposit: evidence for a high $^{18}O$ ore fluid (Canada). Econ. Geol. 83, 1–17.

Bethke, C.M., 1985. A numerical model of compaction-driven groundwater flow and heat transfer and its application to the paleohydrology of intracratonic sedimentary basins. J. Geophys. Res. Solid Earth 90, 6817–6828.

Bleeker, W., Parrish, R.R., 1996. Stratigraphy and U-Pb zircon geochronology of Kidd Creek: implications for the formation of giant volcanogenic massive sulphide deposits and the tectonic history of the Abitibi greenstone belt. Can. J. Earth Sci. 33, 1213–1231.

Bleeker, W., Parrish, R.R., Sager-Kinsman, A., 1999. High-precision U-Pb geochronology of the Late Archean Kidd creek deposit and Kidd volcanic complex. In: Hannington, M.D., Barrie, C.T. (Eds.), Economic Geology Monograph 10: The Giant Kidd Creek Volcanogenic Massive Sulfide Deposit. The Economic Geology Publishing Co., Western Abitibi Subprovince, Canada.

Blomqvist, R.G., 1990. Deep groundwaters in the crystalline basement of Finland, with implications for nuclear waste disposal studies. GFF. 112, 369–374.

Bomberg, M., Nyyssönen, M., Pitkänen, P., Lehtinen, A., Itävaara, M., 2015. Active microbial communities inhabit sulphate-methane interphase in deep bedrock fracture fluids in Olkiluoto, Finland. Biomed. Res. Int. 2015, 979530.

Bottomley, D.J., Ross, J.D., Clarke, W.B., 1984. Helium and neon isotope geochemistry of some ground waters from the Canadian Precambrian Shield. Geochim. Cosmochim. Acta 48, 1973–1985.

Bottomley, D.J., Gascoyne, M., Kamineni, D.C., 1990. The geochemistry, age, and origin of groundwater in a mafic pluton, East Bull Lake, Ontario, Canada. Geochim. Cosmochim. Acta 54, 933–1008.

Bottomley, D.J., Conrad, Gregoire D., Raven, K.G., 1994. Saline ground waters and brines in the Canadian Shield: Geochemical and isotopic evidence for a residual evaporite brine component. Geochim. Cosmochim. Acta 58, 1483–1498.

Bottomley, D.J., Katz, A., Chan, L.H., Starinsky, A., Douglas, M., Clark, I.D., Raven, K.G., 1999. The origin and evolution of Canadian Shield brines: Evaporation or freezing of seawater? New lithium isotope and geochemical evidence from the Slave craton. Chem. Geol. 155, 295–320.

Bottomley, D.J., Chan, L.H., Katz, A., Starinsky, A., Clark, I.D., 2003. Lithium Isotope Geochemistry and Origin of Canadian Shield Brines. Groundwater 41 (6), 847–856.

Bottomley, D.J., Clark, I.D., 2004. Potassium and boron co-depletion in Canadian Shield brines: Evidence for diagenetic interactions between marine brines and basin sediments. Chemical Geology 203, 225–236.

Bottomley, D.J., Clark, I.D., Battye, N., Kotzer, T., 2005. Geochemical and isotopic evidence for a genetic link between Canadian Shield brines, dolomitization in the Western Canada Sedimentary Basin, and Devonian calcium-chloridic seawater. Can. J. Earth Sci. 42, 2059–2071.

Bucher, K., Stober, F.M., 2000. The composition of groundwater in the continental crystalline crust. In: Stober, I., Bucher, K. (Eds.), Hydrogeology of Crystalline Rocks, Water Science and Technology Library, Vol 34. Springer, pp. 205–226.
Clark, I., 2015. Groundwater Geochemistry and Isotopes. CRC Press, 438 pp.
Clark, I.D., Fritz, P., 1997. Environmental Isotopes in Hydrogeology. CRC Press, 328 pp.
Craig, H., 1961. Isotopic variations in meteoric waters. Science 133, 1702–1703.
Eiler, J.M., 2001. Oxygen isotope variations of basaltic lavas and upper mantle rocks. Rev. Mineral. Geochem. 43, 319–364.
Epstein, S., Mayeda, T., 1953. Variation of $^{18}O$ Content of Waters from Natural sources. Geochim. Cosmochim. Acta 4, 213–224.
Fontes, J.C., Fritz, P., Louvat, D., Michelot, J.L., 1989. Aqueous sulphates from the Stripa groundwater system. Geochim. Cosmochim. Acta 53, 1783–1789.
Frape, S.K., Fritz, P., 1982. The chemistry and isotopic composition of saline groundwaters from the Sudbury Basin, Ontario. Can. J. Earth Sci. 19, 645–661.
Frape, S.K., Fritz, P., Mcnutt, R.H., 1984. Water rock interaction and chemistry of groundwaters from the Canadian shield. Geochim. Cosmochim. Acta 48, 1617–1627.
Frape, S.K., Blyth, A.M., Blomqvist, R., McNutt, R.H., Gascoyne, M., 2003. 5.17 - Deep fluids in the continents II. Crystalline rocks. In: Holland, H.D., Turekian, K.H. (Eds.), Treatise on Geochemistry. Pergamon, pp. 541–580.
Frape, S.K., Blyth, A.M., Stotler, R.L., Ruskeeniemi, T., Blomqvist, R., McNutt, R.H., Gascoyne, M., 2014. 7.15 - Deep fluids in the continents. In: Holland, H.D., Turekian, K.H. (Eds.), Treatise on Geochemistry, Second edition. Elsevier, pp. 517–562.
Fritz, P., Frape, S.K., 1982. Saline groundwaters in the Canadian shield a 1st overview. Chem. Geol. 36, 179–190.
Fritz, P., Frape, S.K., Drimmie, R.J., Heemskerk, A.R., 1986. Reply to comments by Grabczak et al. on "Water-rock interaction and chemistry of groundwaters from the Canadian Shield". Geochim. Cosmochim. Acta 50, 1561–1563.
Garrels, R.M., 1984. Genesis of some ground waters from igneous rocks. In: Ableson, P.H. (Ed.), Researches in Geochemistry, Volume 2. Wiley, pp. 405–420.
Goodwin, A.M., 1996. Chapter 1 - Distribution and Tectonic setting of Precambrian crust. In: Goodwin, A.M. (Ed.), Principles of Precambrian Geology. Academic Press, London, pp. 1–50.
Greene, S., Battye, N., Clark, I., Kotzer, T., Bottomley, D., 2008. Canadian shield brine from the con mine, Yellowknife, NT, Canada: noble gas evidence for an evaporated Palaeozoic seawater origin mixed with glacial meltwater and Holocene recharge. Geochim. Cosmochim. Acta 72, 4008–4019.
Grové, D., Harris, C., 2010. O- and H-isotope study of the carbon leader reef at the Tau Tona and Savuka mines (western deep levels), South Africa: implications for the origin and evolution of Witwatersrand Basin fluids. South African J. Geol. 113, 73–86.
Guha, J., Kanwar, R., 1987. Vug brines- fluid inclusions: a key to the understanding of secondary gold enrichment processes and the evolution of deep brines in the Canadian Shield. In: Fritz, P., Frape, S.K. (Eds.), Saline Waters and Gases in Crystalline Rocks GAC Special Paper 33, pp. 95–101.
Heard, A.W., Warr, O., Borgonie, G., Linage, B., Kuloyo, O., Fellowes, J.W., Magnabosco, C., Lau, M.C.Y., Erasmus, M., Cason, E.D., van Heerden, E., Kieft, T.L., Mabry, J.C., Onstott, T.C., Sherwood Lollar, B., Ballentine, C.J., 2018. South African crustal fracture fluids preserve paleometeoric water signatures for up to tens of millions of years. Chem. Geol. 493, 379–395.
Herut, B., Starinsky, A., Katz, A., Bein, A., 1990. The role of seawater freezing in the formation of subsurface brines. Geochim. Cosmochim. Acta 54, 13–21.
Holland, G., Sherwood Lollar, B., Li, L., Lacrampe-Couloume, G., Slater, G.F., Ballentine, C.J., 2013. Deep fracture fluids isolated in the crust since the Precambrian era. Nature 497, 357–360.
Horita, J., Gat, J.R., 1988. Procedure for the Hydrogen Isotope Analysis of Water from Concentrated Brines. Chem. Geol. 72, 85–88.
Huston, D.L., Taylor, B.E., 1999. (1999) Genetic significance of oxygen and hydrogen isotope variations at the Kidd creek volcanic-hosted massive sulfide deposit, Ontario, Canada. In: Hannington, M.D., Barrie, C.T. (Eds.), Economic Geology Monograph 10: The Giant Kidd Creek Volcanogenic Massive Sulfide Deposit. The Economic Geology Publishing Co., Western Abitibi Subprovince, Canada.
Karolytė, R., Serno, S., Johnson, G., Gilfillan, S.M.V., 2017. The influence of oxygen isotope exchange between $CO_2$ and $H_2O$ in natural $CO_2$-rich spring waters: Implications for geothermometry. Appl. Geochem. 84, 173–186.
Kawabe, I., 1978. Calculation of oxygen isotope fractionation in quartz-water system with special reference to the low temperature fractionation. Geochim. Cosmochim. Acta 42, 613–621.
Kelly, W.C., Rye, R.O., Livnat, A., 1986. Saline minewaters of the Keweenaw Peninsula, northern Michigan - Their nature, origin, and relation to similar deep waters in Precambrian crystalline rocks of the Canadian shield. Am. J. Sci. 286, 281–308.
Kerrich, R., Ludden, J., 2000. The role of fluids during formation and evolution of the southern superior province lithosphere: an overview. Can. J. Earth Sci. 37, 135–164.
Kerrich, R., Fryer, B.J., King, R.W., Willmore, L.M., van Hees, E., 1987. Crustal outgassing and LILE enrichment in major lithosphere structures, Archean Abitibi greenstone belt: evidence on the source reservoir from strontium and carbon isotope tracers. Contrib. Mineral. Petrol. 97, 156–168.
Kharaka, Y.K., Hanor, J.S., 2003. 5.16 - Deep fluids in the continents: I. Sedimentary basins. In: Holland, H.D., Turekian, K.H. (Eds.), Treatise on Geochemistry. Pergamon, pp. 1–48.
Kieft, T.L., McCuddy, S.M., Onstott, T.C., Davidson, M., Lin, L.H., Mislowack, B., Pratt, L., Boice, E., Sherwood Lollar, B., Lippmann-Pipke, J., Pfiffner, S.M., Phelps, T.J., Gihring, T., Moser, D., van Heerden, A., 2005. Geochemically generated, energy-rich substrates and indigenous microorganisms in deep, ancient groundwater. Geomicrobiol J. 22, 325–335.
Kietäväinen, R., Ahonen, L., Kukkonen, I.T., Hendriksson, N., Nyyssönen, M., Itävaara, M., 2013. Characterisation and isotopic evolution of saline waters of the Outokumpu deep drill hole, Finland - Implications for water origin and deep terrestrial biosphere. Appl. Geochem. 32, 37–51.
Kietäväinen, R., Ahonen, L., Kukkonen, I.T., Niedermann, S., Wiersberg, T., 2014. Noble gas residence times of saline waters within crystalline bedrock, Outokumpu deep drill hole, Finland. Geochim. Cosmochim. Acta 145, 159–174.
Kietäväinen, R., Ahonen, L., Niinikoski, P., Nykänen, H., Kukkonen, I.T., 2017. Abiotic and biotic controls on methane formation down to 2.5 km depth within the Precambrian Fennoscandian Shield. Geochim. Cosmochim. Acta 202, 124–145.
Kloppmann, W., Girard, J.-P., Négrel, P., 2002. Exotic stable isotope compositions of saline waters and brines from the crystalline basement. Chem. Geol. 184, 49–70.
Knauth, L.P., Epstein, S., 1976. Hydrogen and oxygen isotope ratios in nodular and bedded cherts. Geochim. Cosmochim. Acta 40, 1095–1108.
Kullerud, K., 2000. Occurrence and origin of Cl-rich amphibole and biotite in the Earth's crust - Implications for fluid composition and evolution. In: Stober, I., Bucher, K. (Eds.), Hydrogeology of Crystalline Rocks, Water Science and Technology Library, Vol 34. Springer, pp. 205–226.
Landes, A.A.L., Aquilina, L., Davy, P., Vergnaud-Ayraud, V., Le Carlier, C., 2015. Timescales of regional circulation of saline fluids in continental crystalline rock aquifers (Armorican Massif, western France). Hydrol. Earth Syst. Sci. 19, 1413–1426.
Lau, M.C.Y., Cameron, C., Magnabosco, C., Brown, C.T., Schilkey, F, Grim, S., Hendrickson, S., Pullin, M., Sherwood Lollar, B., van Heerden, E., Kieft, T.L., Onstott, T.C., 2014. Phylogeny and phylogeography of functional genes shared among seven terrestrial subsurface metagenomes reveal N-cycling and microbial evolutionary relationships. Frontiers in Microbiology 5 (531), 1–17.
Lau, M.C.Y., Kieft, T.L., Kuloyo, O., Linage-Alvarez, B., van Heerden, E., Lindsay, M.R., Magnabosco, C., Wang, W., Wiggins, J.B., Guo, L., Perlman, D.H., Kyin, S., Shwe, H. H., Harris, R.L., Oh, Y., Yi, M.J., Purtschert, R., Slater, G.F., Ono, S., Wei, S., Li, L., Sherwood Lollar, B., Onstott, T.C., 2016. An oligotrophic deep-subsurface community dependent on syntrophy is dominated by sulfur-driven autotrophic denitrifiers. Proc. Natl. Acad. Sci. 113, E7927–E7936.
Li, L., Wing, B.A., Bui, T.H., McDermott, J.M., Slater, G.F., Wei, S., Lacrampe-Couloume, G., Sherwood Lollar, B., 2016. Sulfur mass-independent fractionation in subsurface fracture waters indicates a long-standing sulfur cycle in Precambrian rocks. Nat. Commun. 7, 13252.
Lin, L.H., Slater, G.F., Sherwood Lollar, B., Lacrampe-Couloume, G., Onstott, T.C., 2005. The yield and isotopic composition of radiolytic $H_2$, a potential energy source for the deep subsurface biosphere. Geochim. Cosmochim. Acta 69, 893–903.
Lin, L.H., Wang, P.L., Rumble, D., Lippmann-Pipke, J., Boice, E., Pratt, L.M., Sherwood Lollar, B., Brodie, E.L., Hazen, T.C., Andersen, G.L., DeSantis, T.Z., Moser, D.P., Kershaw, D., Onstott, T.C., 2006. Long-term sustainability of a high-energy, low-diversity crustal biome. Science 314, 479–482.
Lippmann, J., Stute, M., Torgersen, T., Moser, D.P., Hall, J.A., Lin, L., Borcsik, M., Bellamy, R.E.S., Onstott, T.C., 2003. Dating ultra-deep mine waters with noble gases and 36Cl, Witwatersrand Basin, South Africa. Geochim. Cosmochim. Acta 67, 4597–4619.
Lippmann-Pipke, J., Sherwood Lollar, B., Niedermann, S., Stroncik, N.A., Naumann, R., van Heerden, E., Onstott, T.C., 2011. Neon identifies two billion year old fluid component in Kaapvaal Craton. Chem. Geol. 283, 287–296.
Lollar, G.S., Warr, O., Telling, J., Osburn, M.R., Sherwood Lollar, B., 2019. 'Follow the Water': hydrogeochemical constraints on microbial investigations 2.4 km below surface at the Kidd creek deep fluid and deep life observatory. Geomicrobiol J. 1–14.
Longstaffe, F.J., Gower, C.F., 1983. Oxygen-isotope geochemistry of Archean granitoid gneisses and related rocks in the English River Subprovince, northwestern Ontario. Precambrian Res. 22, 203–218.
Michalski, J.R., Onstott, T.C., Mojzsis, S.J., Mustard, J., Chan, Q.H.S., Niles, P.B., Johnson, S.S., 2018. The Martian subsurface as a potential window into the origin of life. Nat. Geosci. 11, 21–26.
Miettinen, H., Kietäväinen, R., Sohlberg, E., Numminen, M., Ahonen, L., Itävaara, M., 2015. Microbiome composition and geochemical characteristics of deep subsurface high-pressure environment, Pyhäsalmi mine Finland. Front. Microbiol. 6, 1203.
Morrison, J., Brockwell, T., Merren, T., Fourel, F., Phillips, A.M., 2001. On-line high-precision stable hydrogen isotopic analyses on nanoliter water samples. Anal. Chem. 73, 3570–3575.
Nordstrom, D.K., Lindblom, S., Donahoe, R.J., Barton, C.C., 1989. Fluid inclusions in the Stripa granite and their possible influence on the groundwater chemistry. Geochim. Cosmochim. Acta 53, 1741–1755.
Nurmi, P.A., Kukkonen, I.T., 1986. A new technique for sampling water and gas from deep drill holes (Finland). Can. J. Earth Sci. 23, 1450–1454.
Nurmi, P.A., Kukkonen, I.T., Lahermo, P.W., 1988. Geochemistry and origin of saline groundwaters in the Fennoscandian Shield. Appl. Geochem. 3, 185–203.
O'Neil, J.R., Clayton, R.N., Mayeda, T.K., 1969. Oxygen isotope fractionation in divalent metal carbonates. J. Chem. Phys. 51, 5547.
Onstott, T.C., Lin, L.-H., Davidson, M., Mislowack, B., Borcsik, M., Hall, J., Slater, G., Ward, J., Sherwood Lollar, B., Lippmann-Pipke, J., Boice, E., Pratt, L.M., Pfiffner, S., Moser, D., Gihring, T., Kieft, T.L., Phelps, T.J., Vanheerden, E., Litthaur, D., Deflaun, M., Rothmel, R., Wanger, G., Southam, G., 2006. The origin and age of biogeochemical trends in deep fracture water of the Witwatersrand basin, South Africa. Geomicrobiol J. 23, 369–414.
Piribauer, C., Sindern, S., Meyer, F., Vennemann, T., Prochaska, W., 2011. Fluid inclusions in the Outokumpu deep drill core: implications for palaeofluid evolution and the composition of modern deep saline fluids. Bull. Geol. Surv. Finland 2011, 169–180.
Purkamo, L., Bomberg, M., Nyyssönen, M., Kukkonen, I., Ahonen, L., Kietäväinen, R., Itävaara, M., 2013. Dissecting the deep biosphere: Retrieving authentic microbial

communities from packer-isolated deep crystalline bedrock fracture zones. FEMS Microbiol. Ecol. 85, 324–337.
Schandl, E.S., Wicks, F.J., 1991. Two stages of $CO_2$ metasomatism at the Munro mine, Munro Township, Ontario: evidence from fluid-inclusion, stable-isotope, and mineralogical studies. Can. J. Earth Sci. 28, 721–728.
Sheppard, S.M.F., 1977. Identification of the origin of oreforming solutions by the use of stable isotopes. Geol. Soc. Spec. Publ. 7, 25–41.
Sheppard, S.M.F., 1986. Characterization and isotopic variations in natural waters. Rev. Mineral. Geochem. 16, 165–183.
Sherwood Lollar, B., Frape, S.K., Fritz, P., Macko, S.A., Welhan, J.A., Blomqvist, R., Lahermo, P.W., 1993. Evidence for bacterially generated hydrocarbon gas in Canadian shield and Fennoscandian shield rocks. Geochim. Cosmochim. Acta 57, 5073–5085.
Sherwood Lollar, B., Frape, S.K., Weise, S.M., 1994. New sampling devices for environmental characterization of groundwater and dissolved gas chemistry ($CH_4$, $N_2$, He). Environ. Sci. Technol. 28, 2423–2427.
Sherwood Lollar, B., Westgate, T.D., Ward, J.A., Slater, G.F., Lacrampe-Couloume, G., 2002. Abiogenic formation of alkanes in the Earth's crust as a minor source for global hydrocarbon reservoirs. Nature 416, 522–524.
Sherwood Lollar, B., Voglesonger, K., Lin, L.-H., Lacrampe-Couloume, G., Telling, J., Abrajano, T.A., Onstott, T.C., Pratt, L.M., 2007. Hydrogeologic controls on episodic $H_2$ release from Precambrian fractured rocks—Energy for deep subsurface life on Earth and Mars. Astrobiology 7, 971–986.
Sherwood Lollar, B., Onstott, T.C., Lacrampe-Couloume, G., Ballentine, C.J., 2014. The contribution of the Precambrian continental lithosphere to global $H_2$ production. Nature 516, 379–382.
Simkus, D.N., Slater, G.F., Sherwood Lollar, B., Wilkie, K., Kieft, T.L., Magnabosco, C., Lau, M.C.Y., Pullin, M.J., Hendrickson, S.B., Wommack, K.E., Sakowski, E.G., van Heerden, E., Kuloyo, O., Linage, B., Borgonie, G., Onstott, T.C., 2016. Variations in microbial carbon sources and cycling in the deep continental subsurface. Geochim. Cosmochim. Acta 173, 264–283.
Smith, P.E., Schandl, E.S., York, D., 1993. Timing of metasomatic alteration of the Archean Kidd Creek massive sulfide deposit, Ontario, using $^{40}$Ar- $^{39}$Ar laser dating of single crystals of fuchsite. Econ. Geol. 88, 1636–1642.
Starinsky, A., Katz, A., 2003. The formation of natural cryogenic brines. Geochim. Cosmochim. Acta 67, 1475–1484.
Stotler, R.L., Frape, S.K., Ruskeeniemi, T., Ahonen, L., Onstott, T.C., Hobbs, M.Y., 2009. Hydrogeochemistry of groundwaters in and below the base of thick permafrost at Lupin, Nunavut, Canada. J. Hydrol. 373, 80–95.
Stotler, R.L., Frape, S.K., Freifeld, B.M., Holden, B., Onstott, T.C., Ruskeeniemi, T., Chan, E., 2011. Hydrogeology, chemical and microbial activity measurement through deep permafrost. Ground Water 49, 348–364.
Stotler, R.L., Frape, S.K., Ruskeeniemi, T., Pitkänen, P., Blowes, D.W., 2012. The interglacial-glacial cycle and geochemical evolution of Canadian and Fennoscandian Shield groundwaters. Geochim. Cosmochim. Acta 76, 45–67.
Tarnas, J.D., Mustard, J.F., Sherwood Lollar, B., Bramble, M.S., Cannon, K.M., Palumbo, A.M., Plesa, A.-C., 2018. Radiolytic $H_2$ production on Noachian Mars: implications for habitability and atmospheric warming. Earth Planet. Sci. Lett. 502, 133–145.
Taylor, H.P., 1974. The application of oxygen and hydrogen isotope studies to problems of hydrothermal alteration and ore deposition. Econ. Geol. 69, 843–883.
Taylor, H.P., 1978. Oxygen and hydrogen isotope studies of plutonic granitic rocks. Earth Planet. Sci. Lett. 38, 177–210.
Telling, J., Voglesonger, K., Sutcliffe, C.N., Lacrampe-Couloume, G., Edwards, E., Sherwood Lollar, B., 2018. Bioenergetic constraints on microbial hydrogen utilization in Precambrian deep crustal fracture fluids. Geomicrobiol J. 35, 108–119.
Thurston, P.C., Ayer, J.A., Goutier, J., Hamilton, M.A., 2008. Depositional gaps in Abitibi greenstone belt stratigraphy: a key to exploration for syngenetic mineralization. Econ. Geol. 103, 1097–1134.
Vovk, I.F., 1987. Radiolytic salt enrichment and brines in the crystalline basement of the East European Platform. In: Fritz, P., Frape, S.K. (Eds.), Saline Waters and Gases in Crystalline Rocks GAC Special Paper 33, pp. 197–210.
Ward, J.A., Slater, G.F., Moser, D.P., Lin, L.H., Lacrampe-Couloume, G., Bonin, A.S., Davidson, M., Hall, J.A., Mislowack, B., Bellamy, R.E.S., Onstott, T.C., Sherwood Lollar, B., 2004. Microbial hydrocarbon gases in the Witwatersrand Basin, South Africa: implications for the deep biosphere. Geochim. Cosmochim. Acta 68, 3239–3250.
Warr, O., Sherwood Lollar, B., Fellowes, J., Sutcliffe, C.N., McDermott, J.M., Holland, G., Mabry, J.C., Ballentine, C.J., 2018. Tracing ancient hydrogeological fracture network age and compartmentalisation using noble gases. Geochim. Cosmochim. Acta 222, 340–362.
Warr, O., Giunta, T., Ballentine, C.J., Sherwood Lollar, B., 2019. Mechanisms and rates of $^4$He, $^{40}$Ar, and $H_2$ production and accumulation in fracture fluids in Precambrian Shield environments. Chem. Geol. 530, 119322.
White, D., 1965. Saline water in sedimentary rocks. Am. Assoc. Petrol. Geol. Mem. 4, 342–366.
Zhao, B., Robb, L.J., Harris, C., Jordaan, L.J., 2006. Origin of hydrothermal fluids and gold mineralization associated with the Ventersdorp Contact Reef, Witwatersrand Basin, South Africa: Constraints from S, O, and H isotopes. Spec. Pap. Geol. Soc. Am. 405, 333–352.